A CONFIGURATION FOR THE AT COMPACT ARRAY

AT/10.1/036; AT/17.2/003

R.N. Manchester
for AT Configuration Study Group
29 February 1984

1.0 INTRODUCTION

As approved by the Parliamentary Standing Committee on Public Works, the AT consists of "a compact array of six antennas at Culgoora, New south Wales, a seventh antenna at Siding Spring, New south Wales, and the establishment of a long baseline array in combination with the 64 metre radio telescope at Parkes, New South Wales". Furthermore, the description of the compact array as consisting of five mobile antennas located on a 3km east-west rail-track together with a sixth antenna on a short length of track a further 3km from the western end of the 3km was contained in the proposal approved by the Committee.

Since November 1982 a group known as the AT Configuration Study Group (ATCSG) has been studying the problem of optimizing the configuration of the AT arrays. The membership of the ATCSG has varied since its formation and has included:

G.A. Dulk	R.P. Norris
M.J. Kesteven	D.I. Ostry
M.M. Komesaroff	J.D. O'Sullivan
D.J. McLean	G.T. Poulton
R.N. Manchester (Chairman)	J.A. Roberts
P.J. Napier	P.G. Rogers
	P.R. Wild

In this report the recommendation of the ATCSG on the layout of the Compact Array is presented. In Section 2, the basic parameters of the design are described. These include the provision both of minimum redundancy grating arrays and of grating arrays with sufficient redundancy to calibrate antenna phase errors. The proposed designs are described in Section 3, synthesized beam cross-sections are given in Section 4 and Section 5 gives the results of simulation studies of array performance. Recommendations for future extensions are given in Section 6.

2.0 BASIC PARAMETERS AND REQUIREMENTS

The proposed configuration for the Compact Array has the following basic parameters:

2.1 East-West linear array

A linear east-west array of 6km overall extent consisting of five antennas on a 3km rail-track and a sixth antenna on a short (~100m) length of rail-track 3km further west is proposed.

As mentioned above, this layout was approved by the Parliamentary Public Works committee and hence is largely non-negotiable. However, the ATCSG concurs with the choice of a linear EW array for the following reasons:

* the AT must complement existing radio telescopes. In particular it cannot afford to compete with the VLA in equatorial zone observations. For a given array cost, the highest resolution at declinations south of -30 deg is obtained from a linear east-west array.

* for an exactly east-west array (or more precisely, an array lying in a plane perpendicular to the Earth's rotation axis), image formation and processing are simplified (cf AT/20.1/005).

Despite this, we foresee that, for operation at high frquencies (especially beyond the capability of the VLA), a two-dimensional array would be extremely valuable. We therefore recommend that provision of antenna access to a north-south spur be provided in the initial design (see Section 6.1 below).

2.2 1.5 and 3km arrays

Optimized configurations with maximum baselines of 1.5 and 3km should be provided within the 3km rail-track. These are required for production of maps of similar resolution at different frequencies (octave separation) and for brightness temperature sensitivity limited observations.

2.3 Grating array

The compact array should be a grating array, that is, all baselines being a multiple of a fixed increment. Non-grating arrays have potentially lower peak sidelobe levels but make it more difficult to recognize out-of-field sources and may make it more difficult to implement new image processing techniques. They also make the provision of redundant baselines (see 2.5 below) more difficult. For 22m diameter antennas, the grating increment should be about 15m. This gives a ratio of grating ring radius (~λ/s, where s is the increment) to primary beam half-power diameter (~ 1.1 λ/D, where D is the antenna diameter) of about 1.3. The grating ring radius is slightly greater than the radius to the first null of the primary beam (~1.4λ/D; the ratio is about 1.05.

2.4 Minimum redundancy configurations

It should be possible to build up baseline coverage in successive days with minimum possible redundancy, that is, a minimum number of repeated baselines. The baseline distribution should be approximately uniform after 4, 8, 12, 16 and 20 different array configurations or "days". Each of the four-day segments used to build up the 20-day sequence should by itself give an approximately uniform distribution.

One-day and two-day sequences giving an approximately uniform or approximately "zoom" baseline distributions should be possible. (A "zoom" array is one in which the length of the nth baseline is given by

$$s_n = \alpha \, s_{n-1}$$

where α is a constant factor greater than 1.0 - see AT/10.1/021.)

For the 1.5 and 3km arrays, complete filling of the array, that is, no missing baselines (except the unit increment) out to the maximum, should be possible.

2.5 Calibration using Redundancy

Several days in which the configuration contains sufficient redundancy to completely determine the antenna phase errors, except for an array-wide phase zero and phase slope, should be provided. Furthermore, there should be a sequence of configurations which have sufficient repeated baselines to allow calibration of antenna phases on each day of the sequence (see AT/10.1/033, AT/10.1/035). After calibration the phase slope may change from one integration period to the next; however, on successive days at the same hour angle, the phase slope should be the same. This reduces to a minimum the number of parameters that self-calibration techniques must be used to adjust.

2.6 Minimum number of stations

For observations the antennas are assumed to be located on fixed pads or "stations". In order to minimize costs, the number of these stations must be kept to a minimum, consistent with satisfying the requirements listed above.

2.7 Minimum antenna travel

For operational reasons, the required antenna travel to change from one day of a sequence to the next should be kept to a minimum. For an antenna speed of 2km/hr (AT/01.13/004), the actual antenna travel time will generally be a small fraction of the total reconfiguration time, so this constraint was considered secondary.

3.0 THE ARRAY DESIGN

3.1 Design Procedure

The basic task in the design process was a multi-parameter optimization which attempts to satisfy as many of the requirements listed in Section 2 as possible. This is a difficult task as many of the requirements are conflicting. The procedure used (cf Poulton, URSI/IAU Symposium on Measurement and Processing for Indirect Imaging, Sydney, 1983) was as follows.

Three days, each with sufficient redundancy to determine antenna errors (cf Section 2.5) were provided for the 3km and 6km arrays (AT/10.1/035). This scheme requires that there be 196 basic increments in the range 0-3km and hence that the increment size be 3000/196 = ~15.306m. It also determined the location of 12 stations in the 0-3km zone and two stations at the "6km point" (at locations 388 and 392, that is, separated by four increments or 61.224m).

Stations were then added in the 1.5-3.0km zone in order to provide complete filling of the 1.5km array (that is, all baselines from 2 to 98 times the basic increment) in the shortest possible time with the minimum number of extra stations. A filled array was achieved in 12 days with a total of 22 stations in this zone (including some of those required for the redundant arrays). The 1.5km array was placed at the western ("3km") end of the rail-track in order to provide a smoother transition between the baseline distribution up to 3km and the distribution in the range 3-6km for the 6km array. The number of simultaneous baselines obtained from correlations amongst the five antennas in the 0-3km zone (5x4/2=10) is twice the number obtained in the range 3-6km by correlating the "6km" antenna with the five antennas in the 0-3km zone.

Further stations were then added in the 0-3km zone in order to provide complete filling of the 3km array in the shortest possible time with the minimum number of extra stations. The time required to fill the array is 25 days and the number of stations required (in the 0-3km zone) is 33.

A further two stations were then added in the 0-3km zone to improve the uniformity of the baseline distribution in the 3-6km zone for the 6km array. this brings the total number of stations in the array to 37 of which 35 are on the 3km rail-track and two are at the 6km point. The locations of these stations are given in Table 3.1:

TABLE 3.1

STATION LOCATIONS FOR THE COMPACT ARRAY

Stn No.	Incr. No.	Dist. (m)	Stn No.	Incr. No.	Dist. (m)
1	0	0.000	20	112	1714.286
2	2	30.612	21	113	1729.592
3	4	61.224	22	128	1959.184
4	6	91.837	23	129	1974.490
5	8	122.449	24	140	2142.857
6	10	153.061	25	147	2250.000
7	12	183.673	26	148	2265.306
8	14	214.286	27	163	2494.898
9	16	244.898	28	168	2571.429
10	32	489.796	29	172	2632.653
11	45	688.776	30	173	2647.959
12	64	979.592	31	182	2785.714
13	84	1285.714	32	189	2892.857
14	98	1500.000	33	190	2908.163
15	100	1530.612	34	195	2984.694
16	102	1561.224	35	196	3000.000
17	109	1668.367	36	388	5938.776
18	110	1683.673	37	392	6000.000
19	111	1698.980			

For each of the arrays the required days of observation were then sorted to provide a baseline distribution which was as uniform as possible after 4 and 8 days for the 1.5km array, after 4,8,12,16 and 20 days for the 3km array, and after 4,8 and 12 days for the 6km array. For the 6km array after 12 days, essentially all the baselines available in the 3-6km range, 54 in all, have been obtained.

The baseline distribution for each independent four-day group was itself required to be relatively uniform. This provides for overlapping scheduling of short and long observations; for example, a 4-day and an 8-day observation could share the same observing time as a single 12-day observation. Other combinations are clearly possible. Plenty of scope exists for choosing one- or two-day observations with an approximately uniform, zoom or other baseline distribution. For example, there are approximately 300,000 different one-day 3km arrays available.

The next step in the design was to search for, select and order configurations for the 3 and 6km arrays which, when observed in sequence after the three one-day redundant arrays, allow continued determination of the antenna phases.

Additional independently redundant configurations for the 3km array are contained within the possible set. Besides the original three independent one-day configurations, a further five such configurations exist. Some of these are based on the set of stations at increment numbers 0,2,4,6,8,10,12,16,32,64 and 128. Many other redundant sets are possible on these stations including five completely redundant sets of spacing 2 increments and one of 4 increments.

For observations of compact sources, it may be desirable to observe with a larger effective baseline increment and hence smaller grating ring radius. For a given number of days (or baselines) this would produce a lower sidelobe level within the grating ring. A sequence with double the basic increment (i.e. 30.612m) which fills in 13 days has been found. Also, a sequence with with quadruple the basic increment which fills except for one baseline in 8 days exists.

It perhaps should be noted that, in general, all antennas move in the change from one "day" to the next. On some occasions one antenna does not move. The 6km antenna generally moves less often than those on the 0-3km track. With careful scheduling of similar observing programs it should generally be possible to leave the antennas in a given configuration for several days. Specifically, the provision of the overlapping sequences described above is designed to increase the mean time between array reconfigurations. With baseline and pointing calibrations, reconfigurations are not likely to take less than about 8 hours, so it is essential that observing sequences last several days for each configuration.

Antenna locations and derived baselines are tabulated for each of the arrays in Appendix 1.

3.2 The 1.5km minimum redundancy array

Figure 3.1 shows the adopted configuration for the 1.5km array. This array lies in the 1.5-3.0 km zone, i.e. the western end of the 3km railtrack. (It is not essential that all baselines lie within this zone; however this condition was imposed to minimise antenna travel.) The array is fully filled (apart from the unobservable unit spacing) after 12 days and has been optimized for uniform baseline distribution at 4 and 8 days. The individual 4-day configurations are shown in Figure 3.2.

For the first two days there are no redundant baselines. The number of observed baselines,

$$MN(N-1)/2$$

where M is the number of days of observation and N is the number of antennas, is generally greater than the number of *different* baselines obtained. The ratio of these two quantities, known as the redundancy factor, is 1.025 on day 4, 1.111 on day 8 and 1.237 on day 12. Only 4 new baselines are obtained on the final day.

Accumulated antenna movement is 125 units of the basic increment after 4 days, 269 units after 8 days and 403 units after 12 days. The largest individual antenna movement is 29 units (444m) on day 12.

3.3 The 3km minimum redundancy array

The adopted configuration for the 3km array is shown in Fig. 3.3. The array requires 25 days to fully fill and has been optimized for uniform coverage at 4,8,12,16 and 20 days. Individual four-day configurations are shown in Fig. 3.4. Coverage in these is reasonably uniform; the largest gap is 23 units in the fifth set. Since we expect that shorter observations will be more common than longer observations, the poorer coverage of this segment should not have any great effect.

The redundancy factor is 1.0 (no redundancy) for the first 4 days, 1.025 on day 8, 1.062 on day 12, 1.081 on day 16, 1.136 on day 20 and 1.282 on day 25. These redundancy factors are very low for a linear array; for example, the extended (14-element) Westerbork array has a redundancy factor of 2.275. Most of the redundancy occurs on the last few days as the fully filled array is approached. For example, only four new baselines are obtained on days 22 and 23, and three on days 24 and 25. For the 4-day segments considered individually, the redundancy remains low.

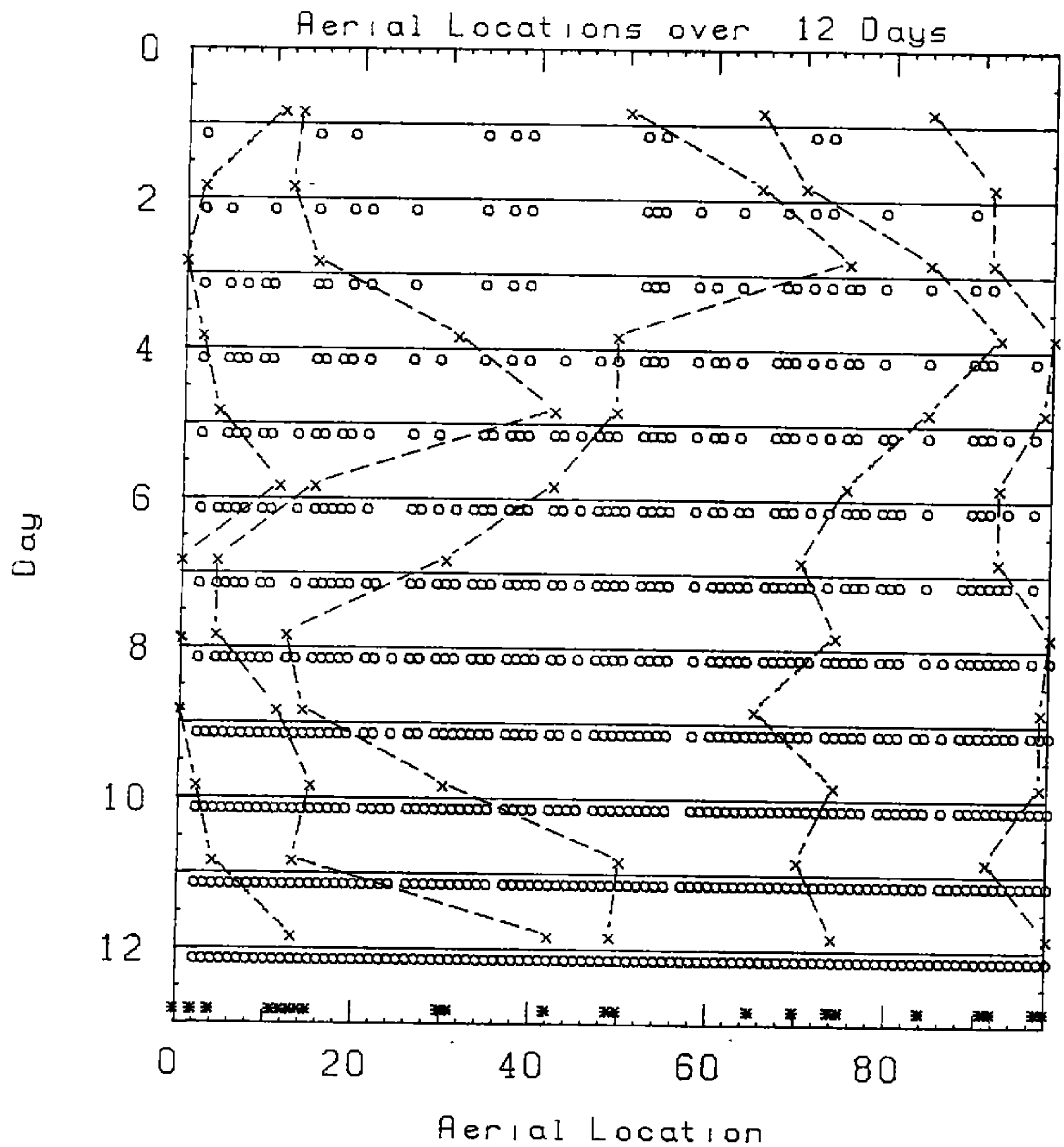

Fig. 3.1 : Antenna locations and the resulting baseline distributions for the 1.5km array. The vertical axis represents day number and the horizontal axis represents both location along the rail track and baseline length. (Note, the eastern end of the array is actually at Station No. 14, Increment No. 98). The five antennas are represented by crosses and the baselines obtained by circles. Antenna positions on successive days are connected by dashed lines and the baseline distribution is cumulative. The station locations are indicated by asterisks along the bottom axis.

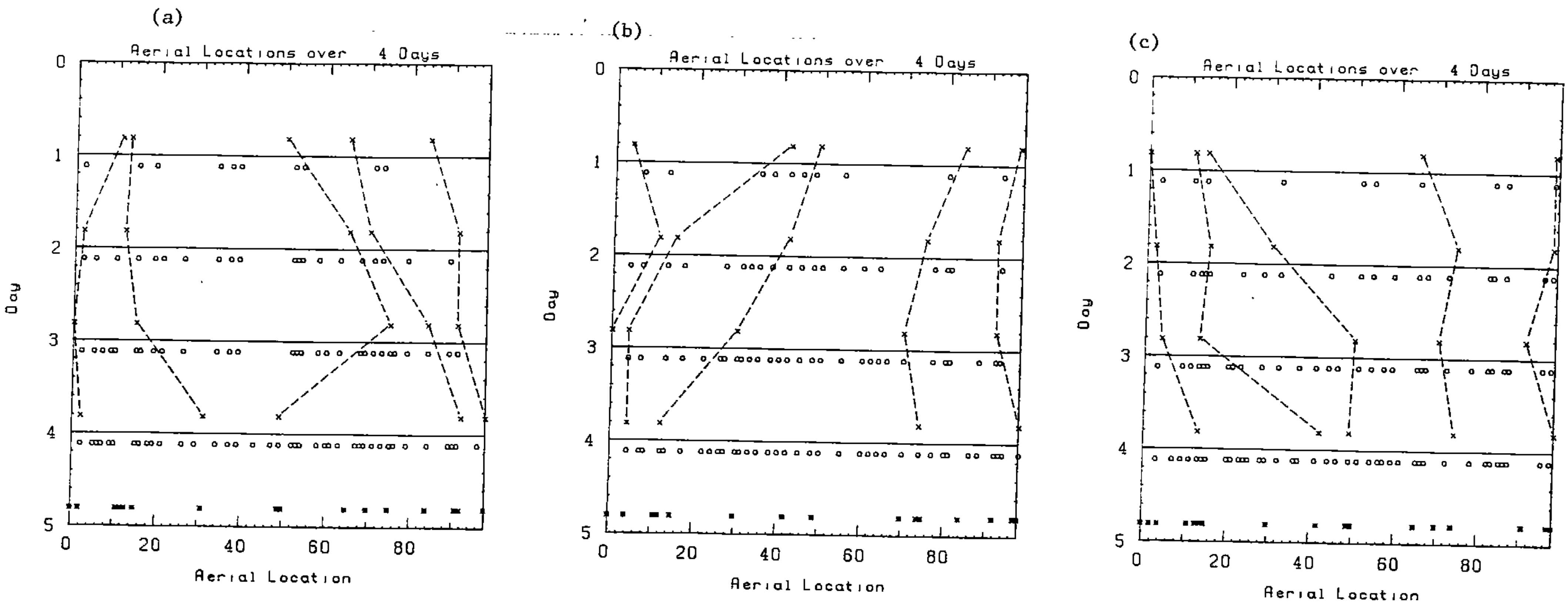

<u>Fig. 3.2</u> : **Antenna locations and baseline distributions for the individual 4-day segments of the 1.5km array configuration. (a) days 1-4; (b) days 5-8; (c) days 9-12.**

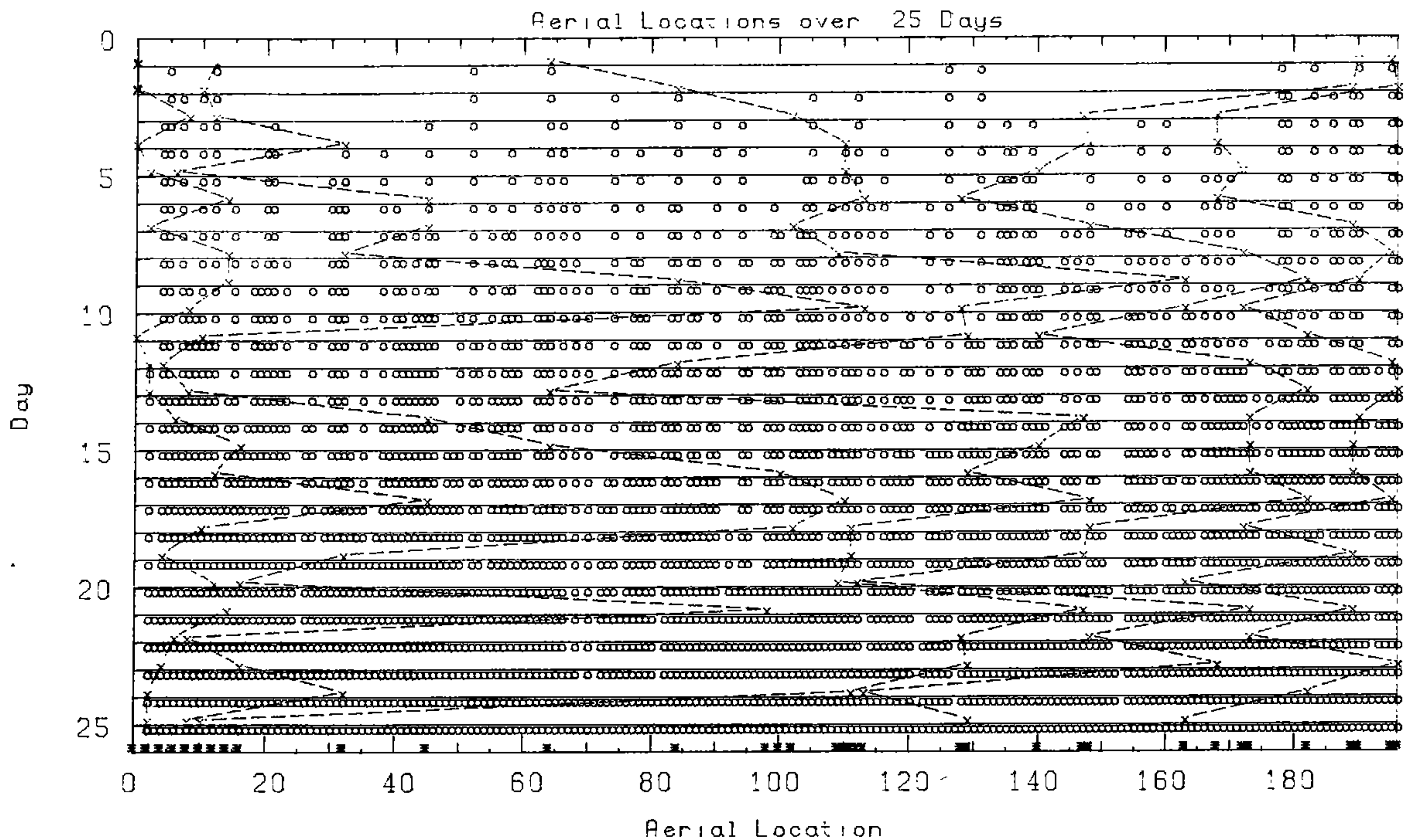

Fig. 3.3 : Antenna and station locations and baseline distributions for the 3km array. There are 35 stations and 196 units of the basic increment across the 3km.

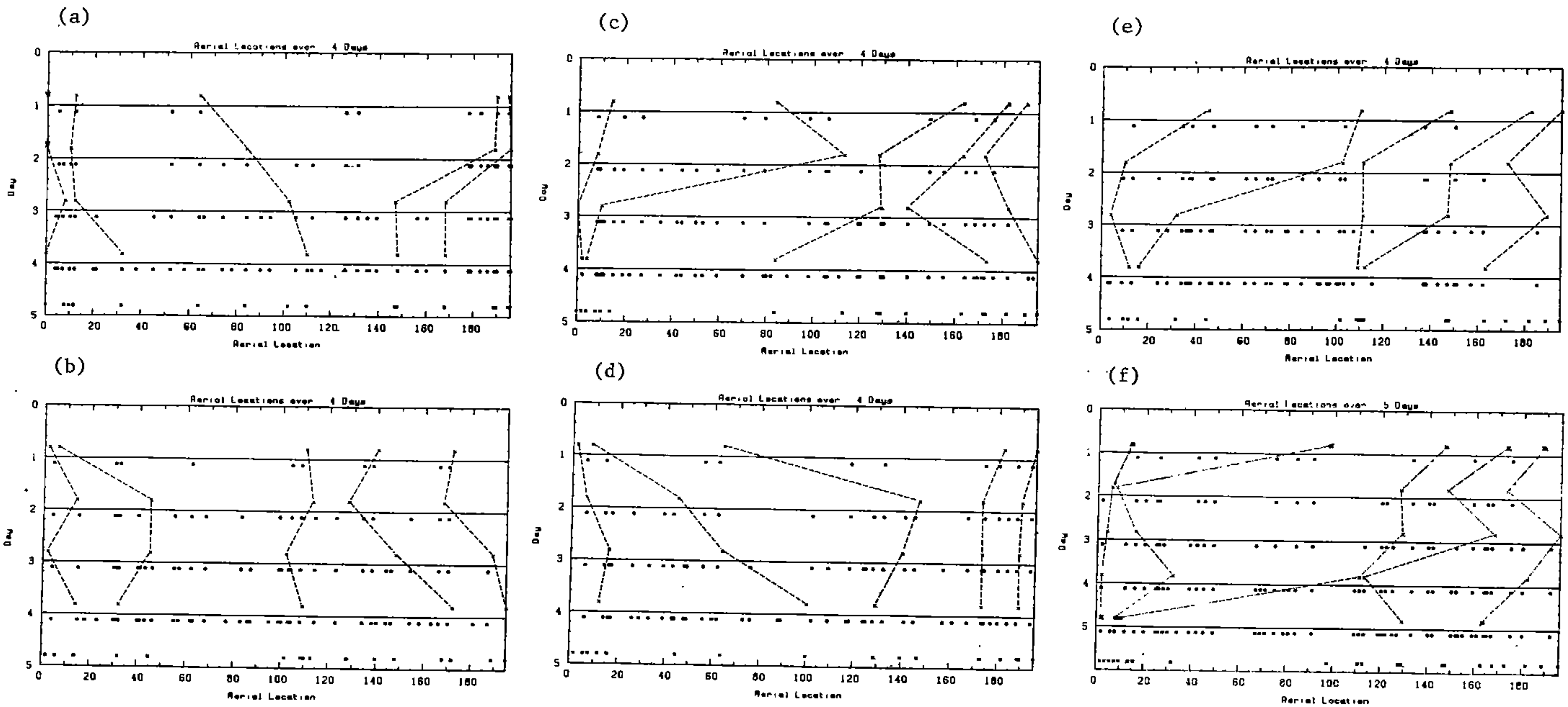

Fig. 3.4 : Antenna locations and baseline distributions for individual 4-day segments of the 3km array configuration. For completeness the plot for the final 5-day segment is also shown. (a) days 1-5; (b) days 5-8; (c) days 9-12; (d) days 13-16; (e) days 17-20; (f) days 21-25.

Accumulated antenna movement is 159,395,867,1128,1523 and 2209 units after 4,8,12,16,20 and 25 days respectively. The largest individual antenna movement is 103 units (1576m) on day 11.

3.4 The 6km minimum redundancy array

The 6km array shown in Figure 3.5 has a different character from the 1.5km and 3km arrays because of the absence of connecting railtrack and hence of stations in the 3 to 6km zone. For five antennas on the 0-3km railtrack and one antenna at the 6km point, the number of observed baselines in the 3-6km range (5 per day) is always half the number in the 0-3km range (10 per day). The maximum number of baselines obtainable in the 3-6km range is the number of stations in the 0-3km zone (35), times the number of stations at (or near) the 6km point (2), that is, 70 in all. In the current design thirteen of these are redundant and the total number of different baselines obtainable is 57. In 12 days, 54 of these non-redundant baselines are obtained, so the effect of further observation is primarily to fill the 0-3km zone. Note that the antenna locations for the 6km sequence are quite different from those for the 3km sequence, so it will not be possible to schedule overlapping 3 and 6km observations. Observations of the 3km sequence with the 6km antenna included produces the less than optimal coverage of the 3-6km zone shown in Figure 3.6. This may be adequate for some purposes.

Because of the clumping of stations in the 0-3km zone, the distribution of baselines in the 3-6km zone is not very uniform. This may be a problem for long observations (> 12 days) of complex fields, for example in the Galactic plane or the Magellanic Clouds, where the resolution of the 6km array is required. The problem could be alleviated by the addition of a third station near the 6km point, for example, at location 383, 9 units or 138m from the 6km point. Given sufficient observing time, this would allow approximately 25 extra baselines to be added in the 3-6km range. Some of the larger holes could also be filled by adding further stations in the 0-3km zone. However this is less effective since only two baselines are added per station.

Baseline distribution diagrams for the three individual 4-day segments of the 12-day sequence (Fig. 3.5) are given in Fig. 3.7. In each case they have been optimized for uniform coverage. By far the largest gap (62 units) is in the third segment. The next largest gap is 29 units in the second segment.

For the first four days of the 12-day sequence shown in Fig. 3.5 there is no redundancy. After 8 days the redundancy factor is 1.043 and after 12 days, 1.065. This latter figure corresponds to 11 repeated baselines out of the 180 observed.

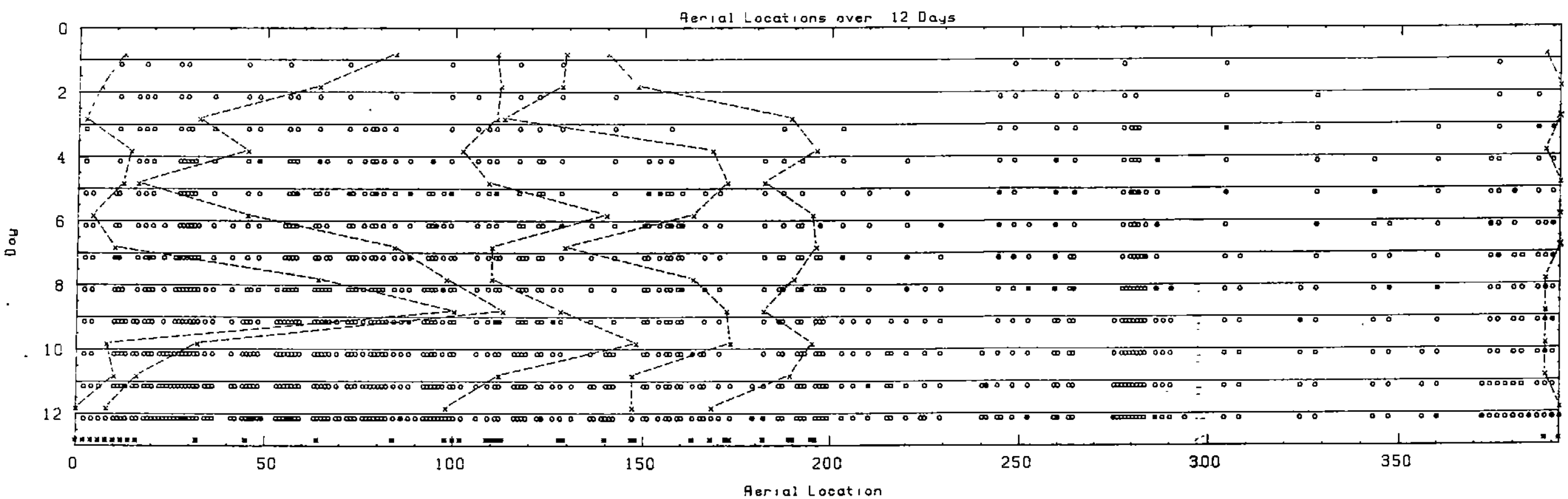

<u>Fig. 3.5</u> : Antenna and station locations and baseline distributions for the optimized 6km array. The 35 stations in the 0-3km (eastern) zone are those of the 3km array (Fig. 3.3) and there are two further stations at locations 388 and 392 near the 6km point.

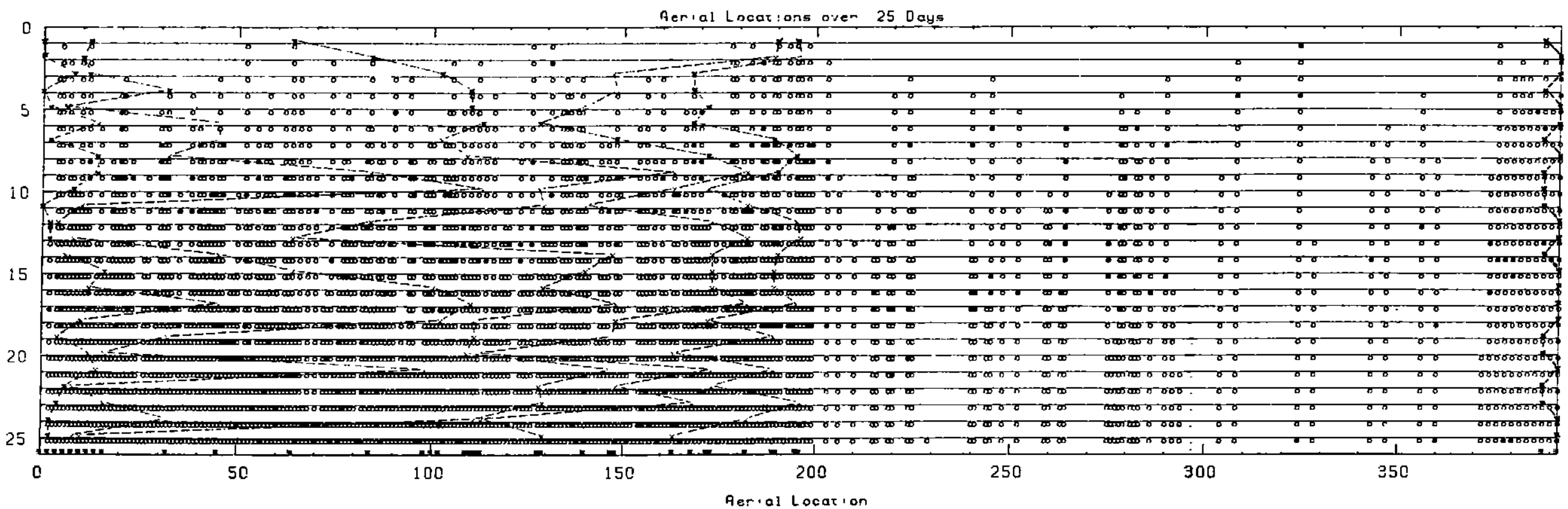

<u>Fig. 3.6</u> : Baseline distributions for the 6km array based on the 25 days of the optimized 3km array.

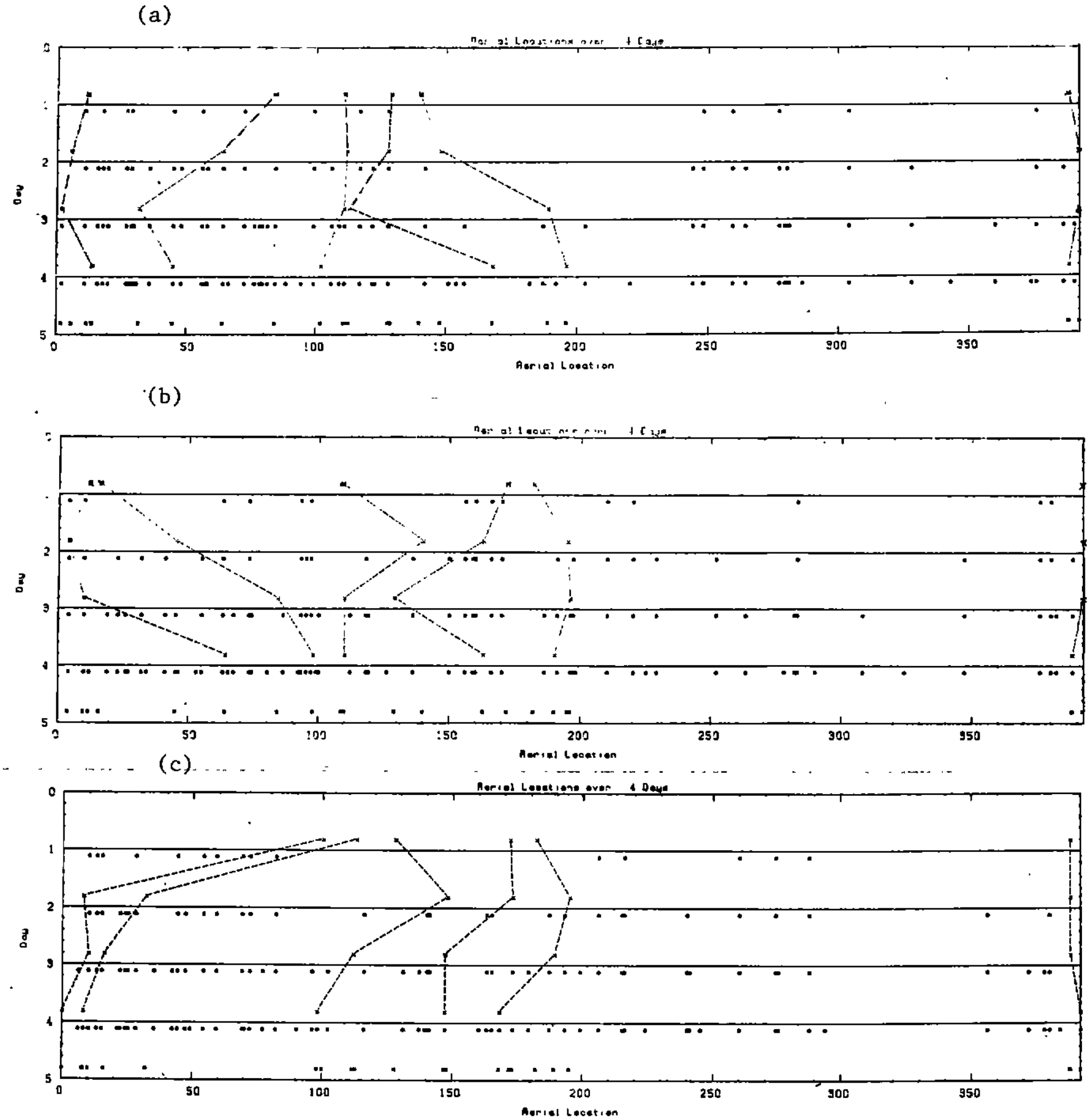

<u>Fig. 3.7</u> : Antenna locations and baseline distributions for the three individual 4-day segments of the optimized 6km array (Fig. 3.5); (a) days 1-4; (b) days 5-8; (c) days 9-12.

Cumulative antenna travel is 223 units after 4 days, 605 units after 8 days and 1041 units after 12 days. The largest individual movement is 92 units (1408m) on day 10.

3.5 The 6km redundant array

Configurations for the 6km array which contain sufficient redundancy to completely determine all antenna phase errors (apart from an arbitrary phase zero and phase slope for each hour angle) are shown in Fig. 3.8. Following the scheme outlined in AT/10.1/035, day 1 is based on the redundant set (-8,0,1,2,4,8) with a basic 24 unit step. In this set the -8 point is placed at the 6km point and the remaining five positions are in the 0-3km zone. Since we need to determine four antenna phase errors (phase errors can be arbitrarily set for two antennas), four baselines in this set are redundant leaving 11 non-redundant baselines.

Day 2 is based on the set (-7,0,1,2,4,7) with a basic 28 unit step which is similarly calibratable. However in order to relate the phase slope to that on day 1, one spacing (7x24 = 6x28 = 168 units) is repeated, giving 10 new spacings. The third day is also based on the set (0,1,2,4,7) in the 0-3km zone with a basic 7 unit step. For the 6km array, this day is not independently calibratable; however by combining it with the first day it can be calibrated giving 10 new baselines. Succeeding days all contain 5 spacings which have been previously observed and hence give 10 new spacings. A total of 11 such days have been found giving a total of 14 days of calibrated observations.

The arbitrary phase errors for each hour angle step must be determined using some procedure such as self-calibration. The redundancy has reduced the number of variables in the self-calibration from 5M, where M is the number of days of integration time, to one per integration time, hence making it more likely that a unique solution can be obtained. One of course pays the penalty that fewer independent baselines are measured; for example, after 12 days one has 121 measured baselines using the redundant scheme (redundancy factor = 1.488) versus 169 measured baselines in the minimally redundant scheme (Section 3.4). However, the number of errors to be determined per integration time by self-calibration has been reduced from 60 to one.

In a sense, the sequence shown in Fig. 3.8 is a minimum redundancy solution in that it contains sufficient redundancy to calibrate the antenna phases but *no more*. A preliminary study of error propagation in the solution showed that this should not be a serious problem.

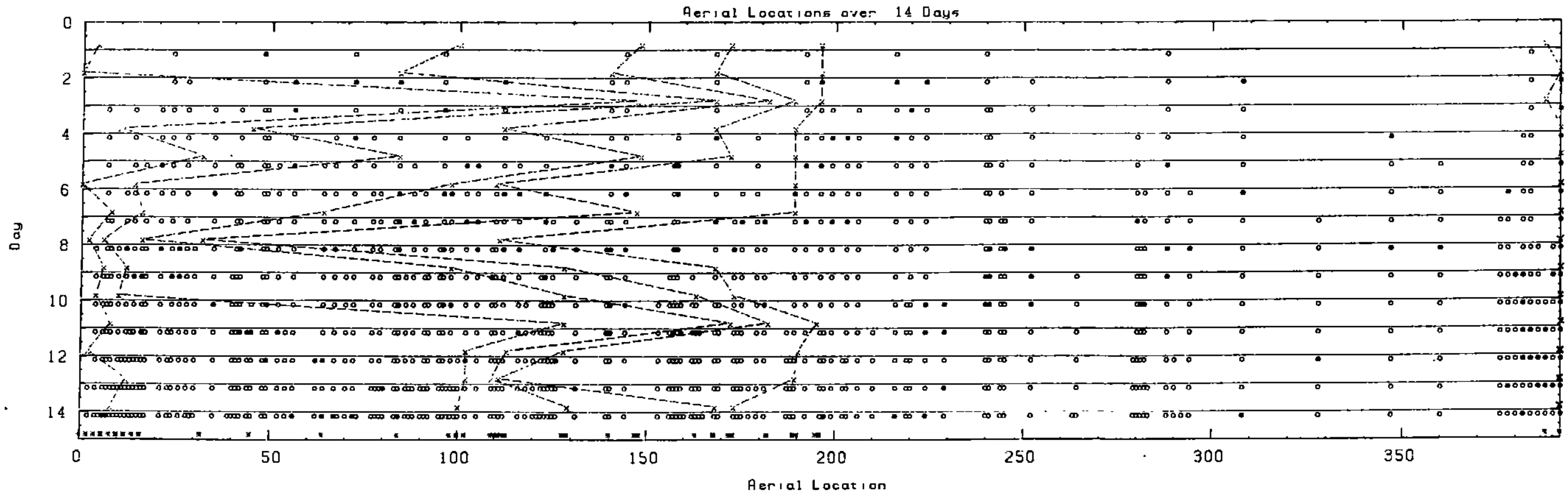

Fig. 3.8 : Antenna locations and baseline distributions for the 6km redundant array.

The sequence shown in Fig. 3.8 is in the order in which the data must be analyzed in order to propagate the calibration. For example, in order to calibrate day 12, days 1-11 must have been observed. However, they need not be observed in this order which involves some relatively long antenna movements (about 2.5km), especially on days 3 and 4. Sorting of these days for minimum antenna travel would reduce the total amount of antenna movement.

3.6 The 3km redundant array

The five antennas in the 0-3km zone for each of the first three days described in the previous section are independently calibratable. Since there are 3 errors that can be determined, on the first day we obtain 7 measured baselines. After that, 6 new baselines per day are obtained since one spacing must be a repeat of one on a previous day in order to relate the phase slopes. Figure 3.9 shows a sequence in which full calibration is maintained for 17 days. In this sequence the redundant spacings are generally fairly long. A different sequence of similar length has been found in which the redundant spacings are typically shorter which may be more suitable for some purposes. As for the 6km sequence described in the previous section, the sequence shown in Fig. 3.9 is in the order in which the data must be analyzed. Some reduction in the total amount of antenna travel would be possible. However, it should be noted that this sequence has the attractive feature that an antenna is stationary on the first station from days 4 to 18.

3.7 The 1.5km redundant array

A number of redundant arrays, in particular day 3 of the 3km set described above, exist within a maximum baseline of 1.5km. However at this time, redundant configurations giving full calibration with a maximum baseline of 1.5km have not been incorporated into the design. A two-dimensional array may be a more useful facility for high frequency observations where self-calibration is especially important.

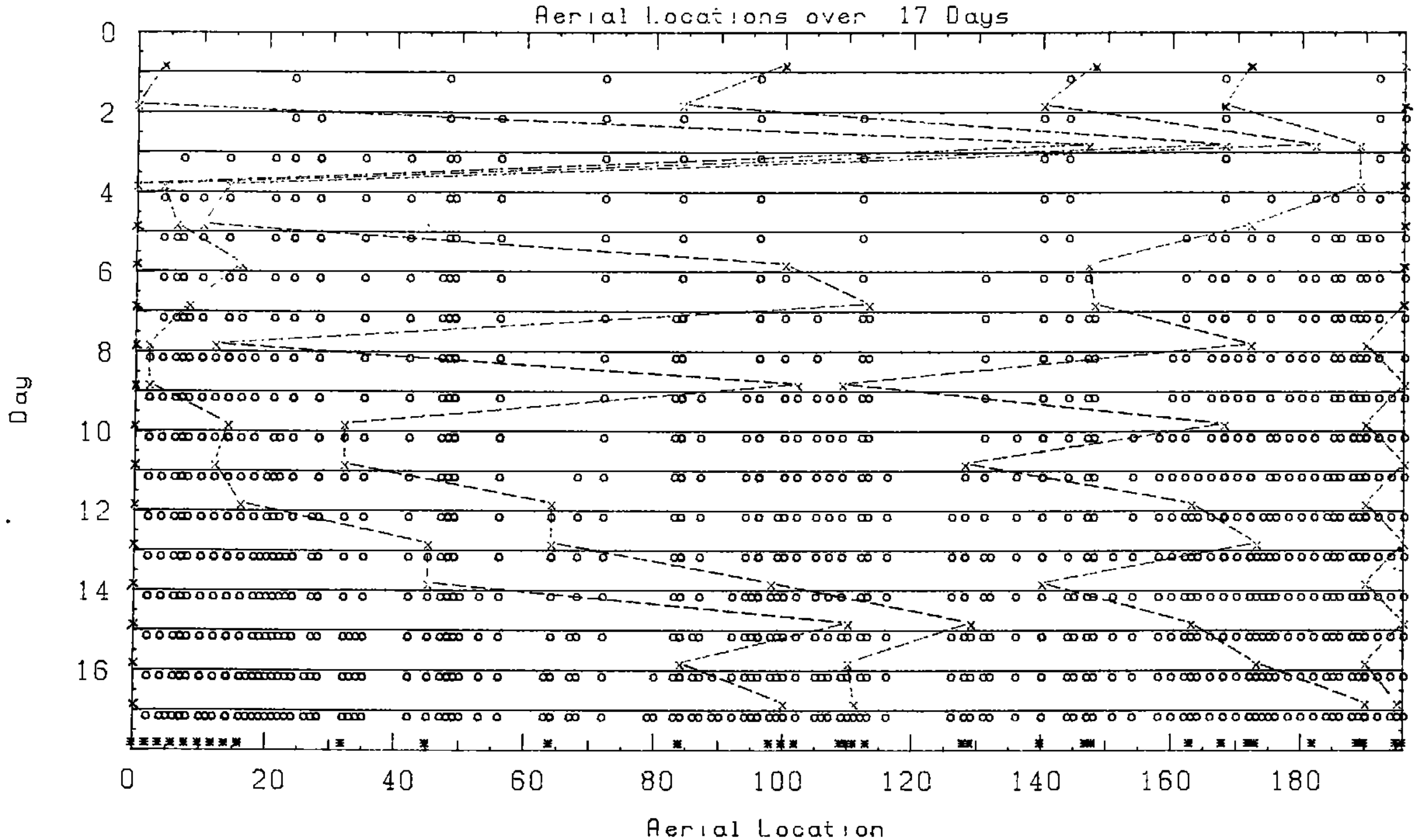

Fig. 3.9 : Antenna locations and baseline distributions for the 3km redundant array.

4.0 SYNTHESIZED BEAM PATTERNS

Synthesized beam patterns have been computed for the minimum redundancy arrays discussed above including the separate 4-day segments and some longer observations. The patterns were computed by direct summing of the Bessel function patterns for each observed baseline. The weighting factor was effectively "uniform", i.e. for a point source, visibilities were of equal amplitude across the u-v plane. All patterns are computed out to the first true grating ring, i.e. the radius corresponding to the increment of 15.306m. For a frequency of 1.4 GHz, the radius of this ring is 47.4'arc. For comparison, with typical illumination taper, the half-power primary beamwidth is about 36'arc and the radius of the first null in the primary beam is about 46'arc. Rms and peak sidelobe levels for the various cases considered are summarized in Table 4.1.

4.1 The 1.5km Minimum Redundancy Array

Figure 4.1 shows the synthesized beam patterns for each of the separate 4-day segments. Outside the near-in sidelobes and the corresponding region around the grating ring the peak sidelobe levels are around -15 dB. The distribution of this "pseudo-grating" structure is somewhat different on each of the 4-day segments but of similar character. The rms sidelobe level in this region is about -20.7 dB for each segment. Since the weighting was effectively uniform, the near-in sidelobes are relatively high, about -10 dB. The level of the first grating ring is about -14 dB.

In Fig. 4.2 synthesized beam patterns are given for an 8-day observation and for the full 12 days, corresponding to complete filling of the array (Fig. 3.1). The principal effect of the increased observing time is to lower the general sidelobe level between the main beam and the grating ring. It is important to note that the level of the grating ring is unaffected by the more complete coverage. Peak sidelobe levels are around -19 dB for the 8-day synthesis, that is, about 4 dB lower than those for 4-day syntheses, and the rms sidelobe level, -23.1 dB, is 2.4 dB less.

For the 12-day synthesis one has the classical pattern for a fully filled array (slightly modified because of the missing unit spacing) which reaches a minimum sidelobe level of about -33 dB at half the grating ring radius. In practice, residual calibration errors will destroy the perfect cancellation which results in these very low sidelobe levels. The degree to which this occurs obviously depends on the magnitude of the errors; for random errors of about one degree of phase, a minimum sidelobe level of about -28 dB would be expected.

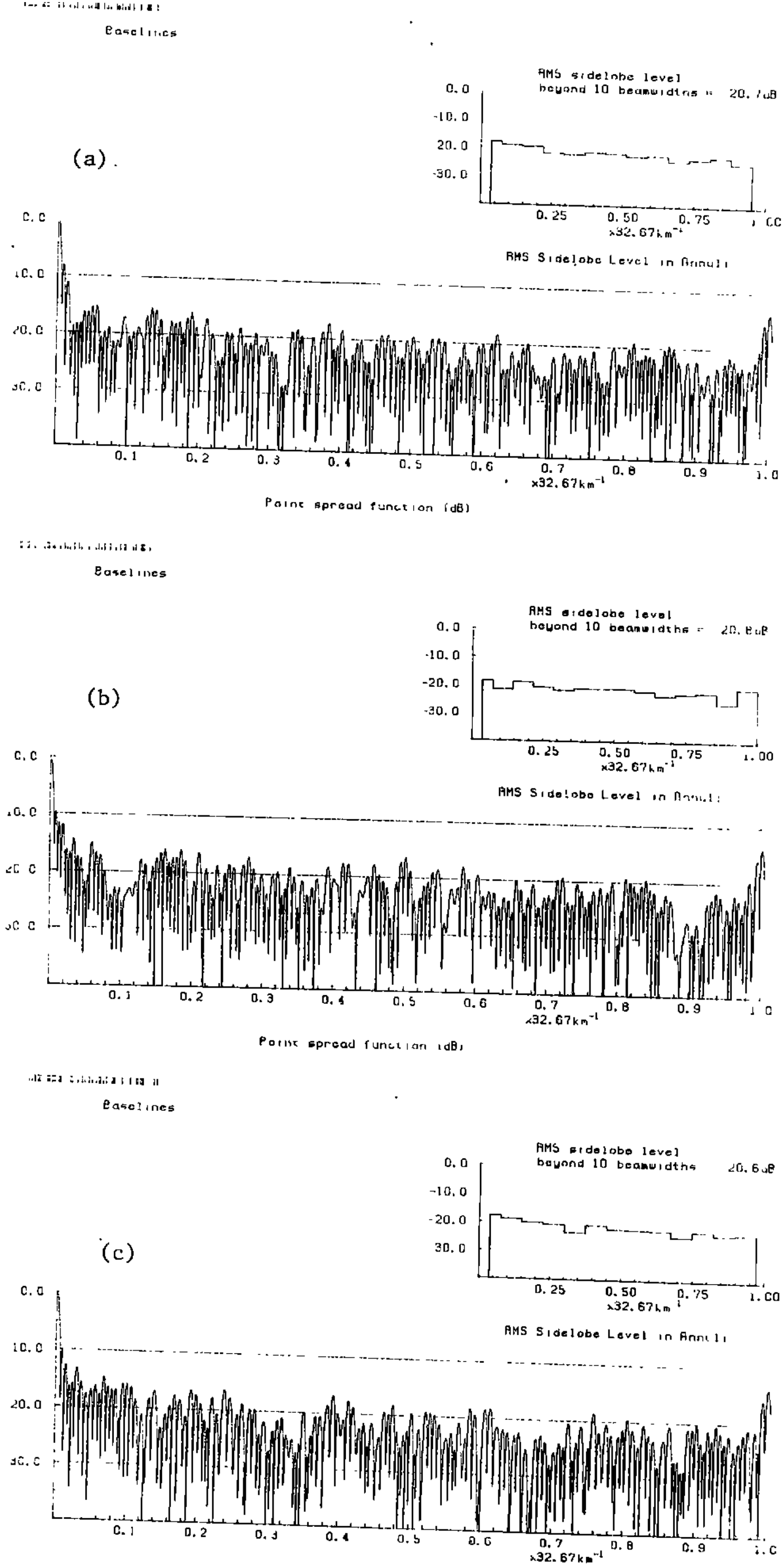

Fig. 4.1 : Synthesized beam patterns out to the first grating ring for the three separate 4-day segments of the observing sequence for the 1.5km array (Fig. 3.1). The vertical axis is logarithmic (the absolute value of the response is plotted) and calibrated in dB, and the horizontal scale is a fraction of the grating ring radius. Average sidelobe levels over radial segments are plotted in the upper right corner and the rms sidelobe level between radii of 10 beamwidths and the grating ring radius minus 10 beamwidths, relative to the main beam is quoted. In computing this average the radial segments were weighted by their area, that is, by radius. In the upper left corner the baseline distribution is indicated. This may be seen more clearly in the appropriate figure of Section 3. (a) Days 1-4; (b) days 5-8; (c) days 9-12.

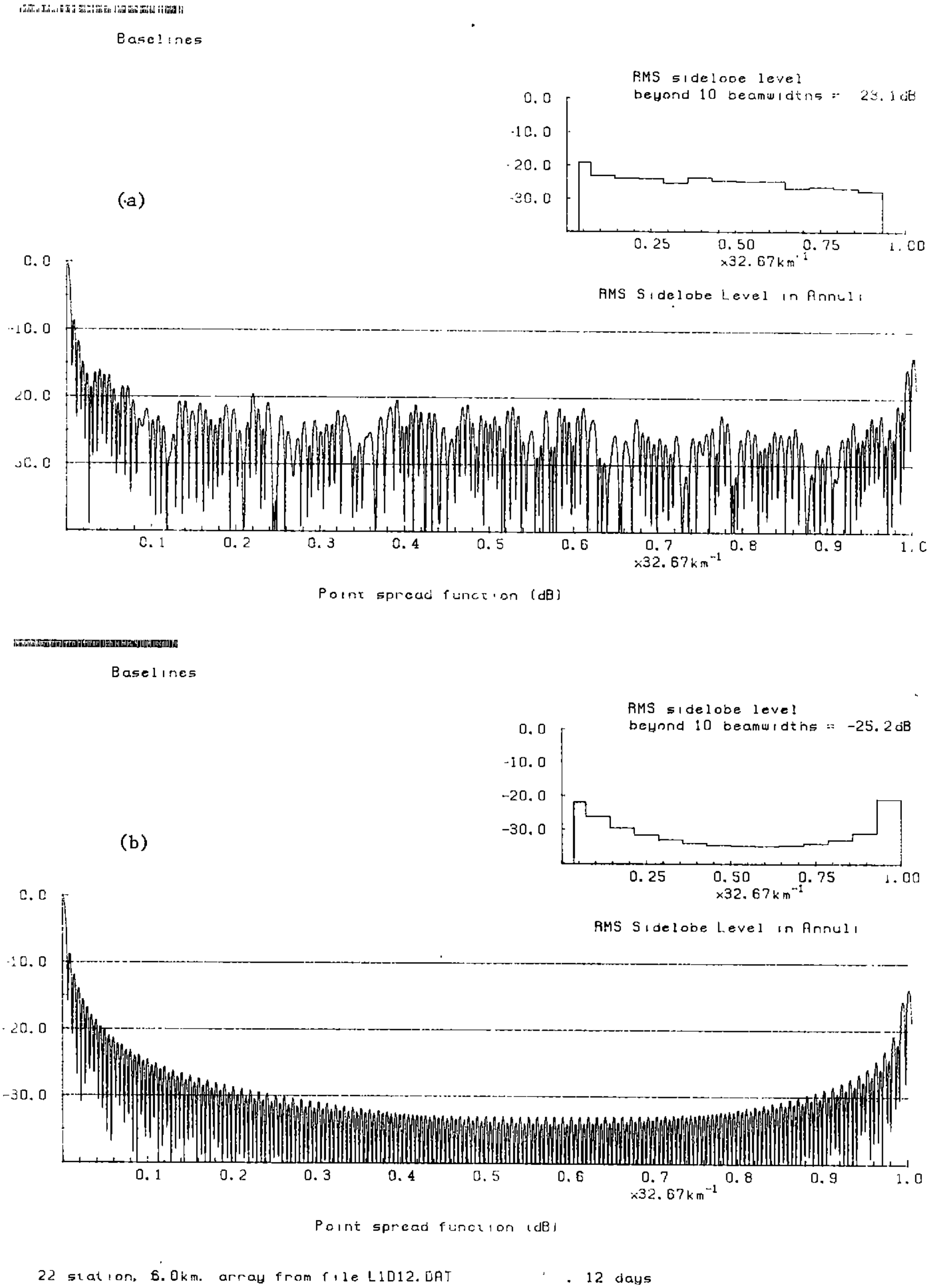

Fig 4.2 : Synthesized beam patterns for the 1.5km minimum redundancy array for (a) days 1-8 and (b) the full 12 days, that is, complete filling of the array.

4.2 The 3km Minimum Redundancy Array

Synthesized beam patterns for the individual 4-day segments out to 20 days and the final 5-day segment for the 3km array are shown in Fig. 4.3. As for the 1.5km array, the patterns for the different 4-day segments differ in detail but have the same overall character. The peak sidelobe levels are about -16 dB and the rms sidelobe levels are about -22 dB, both a little lower than for the 1.5km array. It is interesting to note that the first segment [Fig. 4.3(a)] has a relatively high sidelobe level at 0.5 grating ring radii, corresponding to a periodicity at twice the basic increment, whereas the third and fourth segments [Figs 4.3(c) and (d)] have nulls at this point.

In Fig. 4.4 beam patterns are shown for longer periods of observation. As for the 1.5km array, the main effect of longer observation times is reduction of the average sidelobe level between the main beam and the grating ring. Peak sidelobe levels range between about -17 dB for the 8-day synthesis and -24 dB for the 20-day synthesis. For the fully-filled array the minimum sidelobe level is about -38 dB, 5 dB less than for the 1.5km array; the fully-filled 3km array has twice as many baselines as the fully-filled 1.5km array since the increment is the same for each. The 24-day synthesis has three missing baselines which raises the peak sidelobe level to about -30 dB. This illustrates the effect that out-of-service antennas will have on attempts to completely fill the array. Rms sidelobe levels vary in a corresponding way from -24.3 dB for an 8-day synthesis to -29.2 dB for a 20-day synthesis. For the 24- and 25-day syntheses the rms levels are -31.3 and -32.5 dB respectively.

4.3 The 6km Minimum Redundancy Array

Synthesized beam patterns for separate 4-day segments of the 6km observing sequence are shown in Fig. 4.5. Peak sidelobe levels are generally less than -18 dB with rms values of about -23.5 dB. A fairly strong feature corresponding to the double-increment periodicity is evident. This feature is also clear on the patterns for longer observations shown in Fig. 4.6. The regular set of stations discussed in the final paragraph of Section 3.1, together with the 4-increment spacing of the two stations at the 6km point, would be largely responsible for this periodicity. After 12 days the peak sidelobe levels are generally less than -20 dB and their rms value is -26.9 dB. This is somewhat better than for the corresponding 3km array owing to the larger number of baselines in the 6km array.

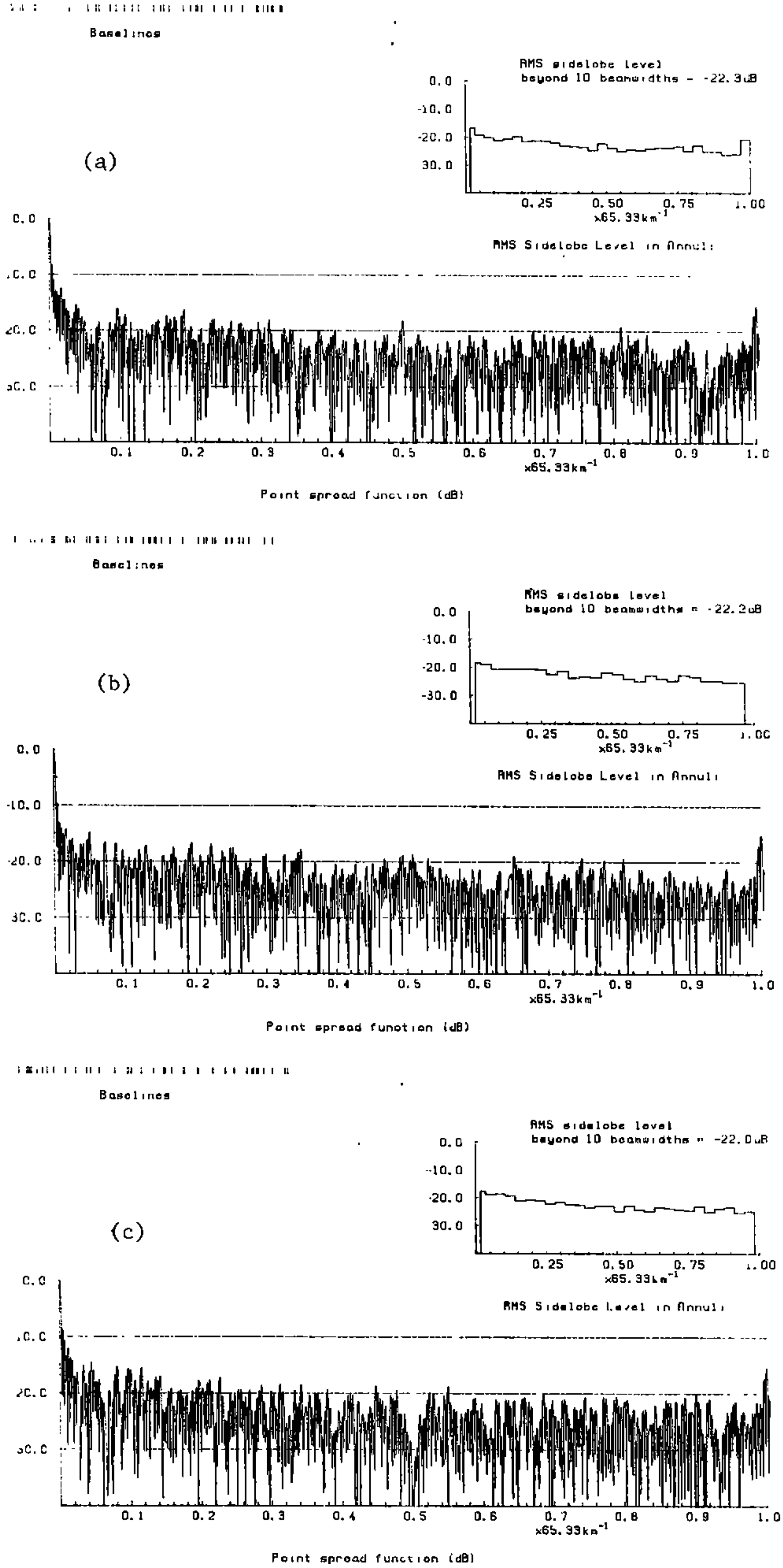

<u>Fig. 4.3</u> : Synthesized beam patterns for the 3km minimum redundancy array. (a) days 1-4; (b) days 5-8; (c) days 9-12'; (d) days 13-16; (e) days 17-20; (f) days 21-25.

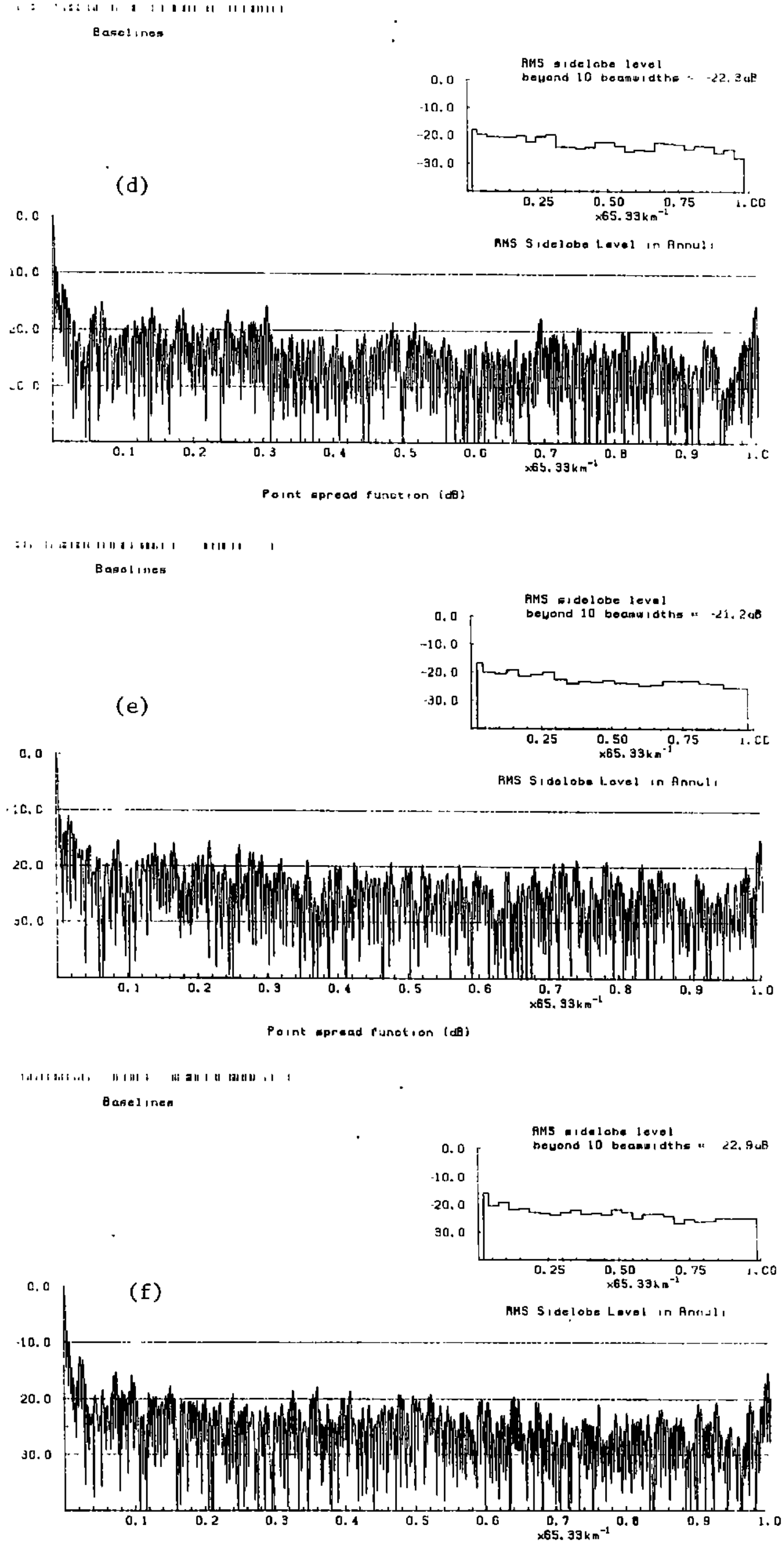

<u>Fig. 4.3</u> : Synthesized beam patterns for the 3km minimum redundancy array. (a) days 1-4; (b) days 5-8; (c) days 9-12; (d) days 13-16; (e) days 17-20; (f) days 21-25.

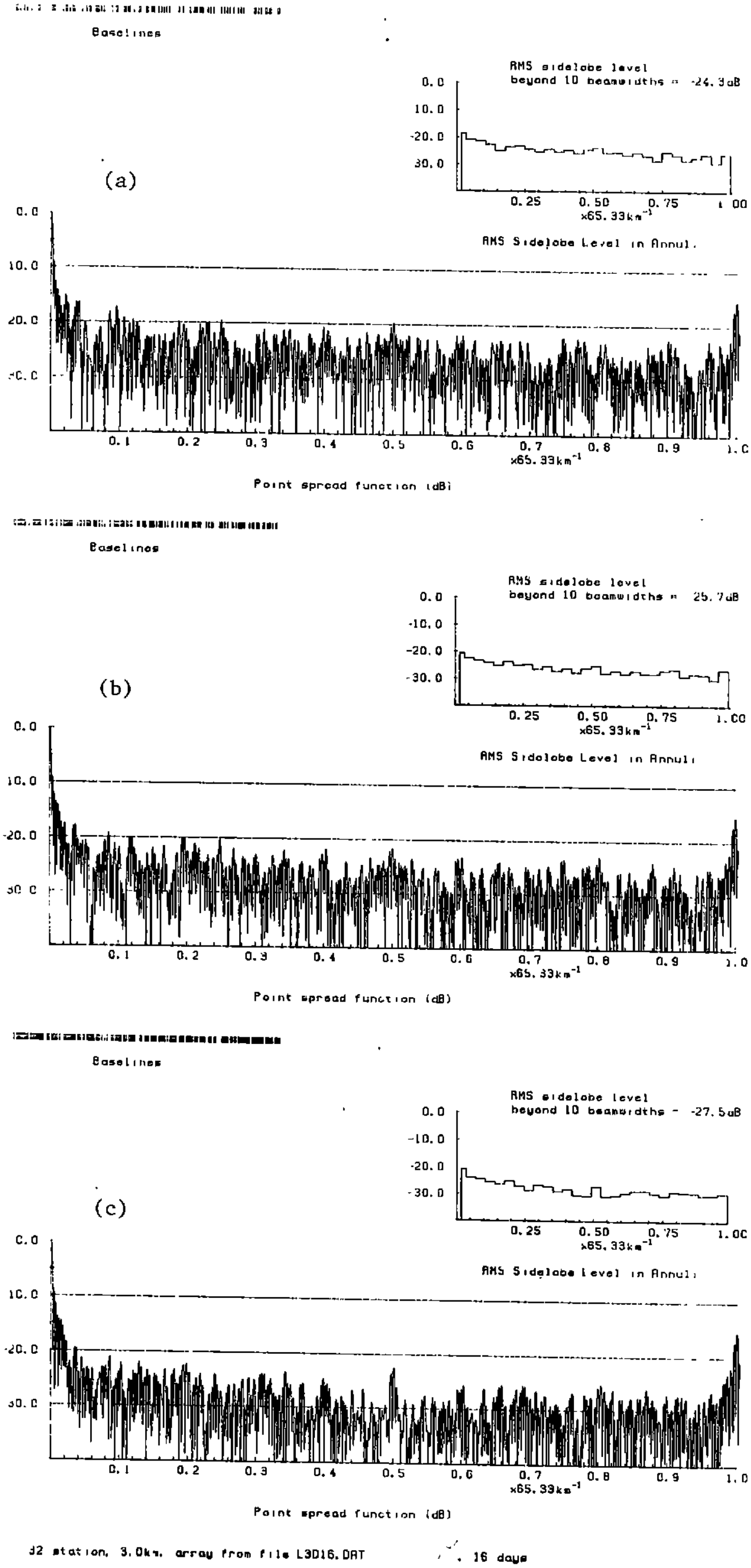

<u>Fig. 4.4</u> : Synthesized beam patterns for longer observations with the 3km minimum redundancy array. (a) days 1-8; (b) days 1-12; (c) days 1-16; (d) days 1-20; (e) days 1-24; (f) days 1-25.

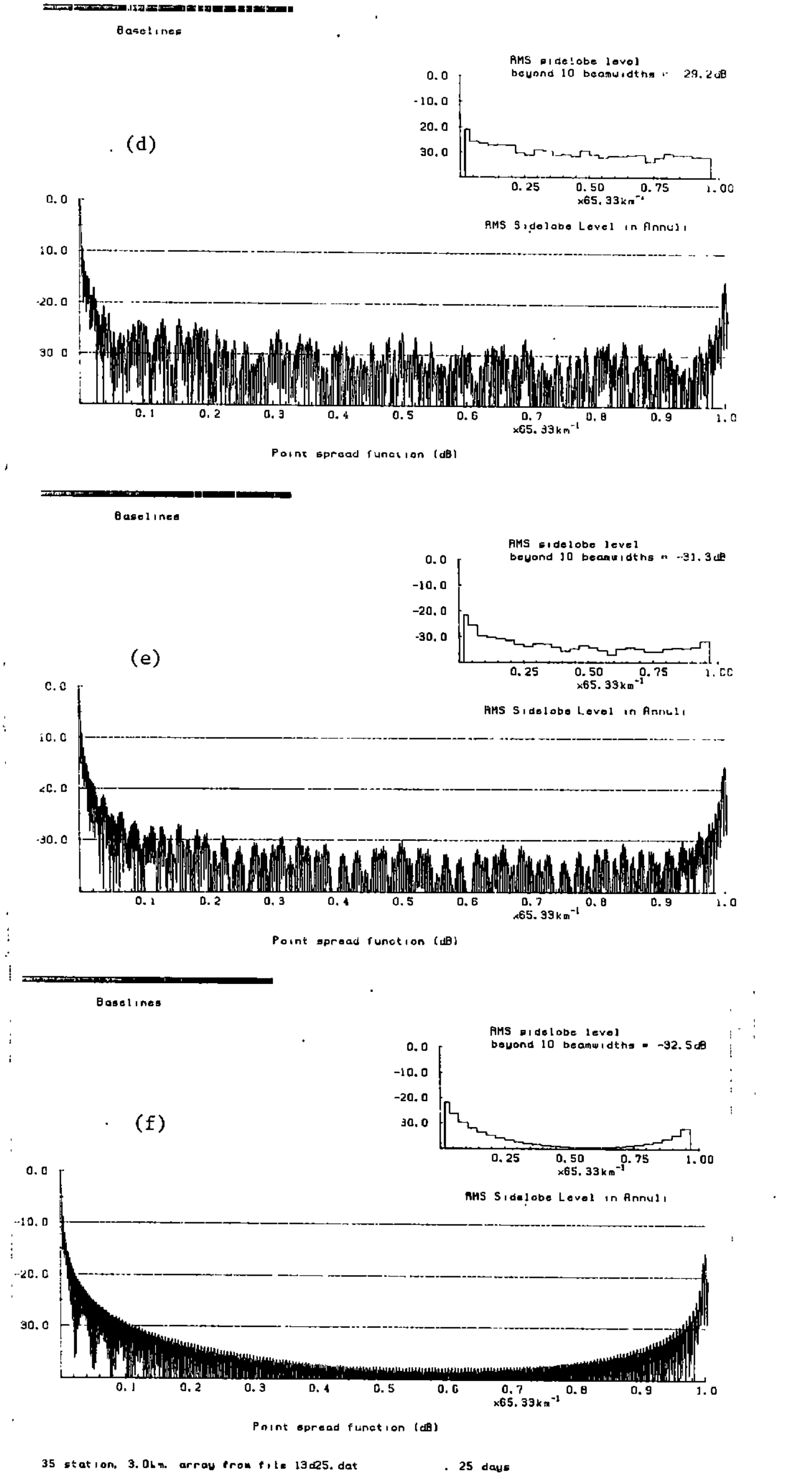

Fig. 4.4 : Synthesized beam patterns for longer observations with the 3km minimum redundancy array. (a) days 1-8; (b) days 1-12; (c) days 1-16; (d) days 1-20; (e) days 1-24; (f) days 1-25.

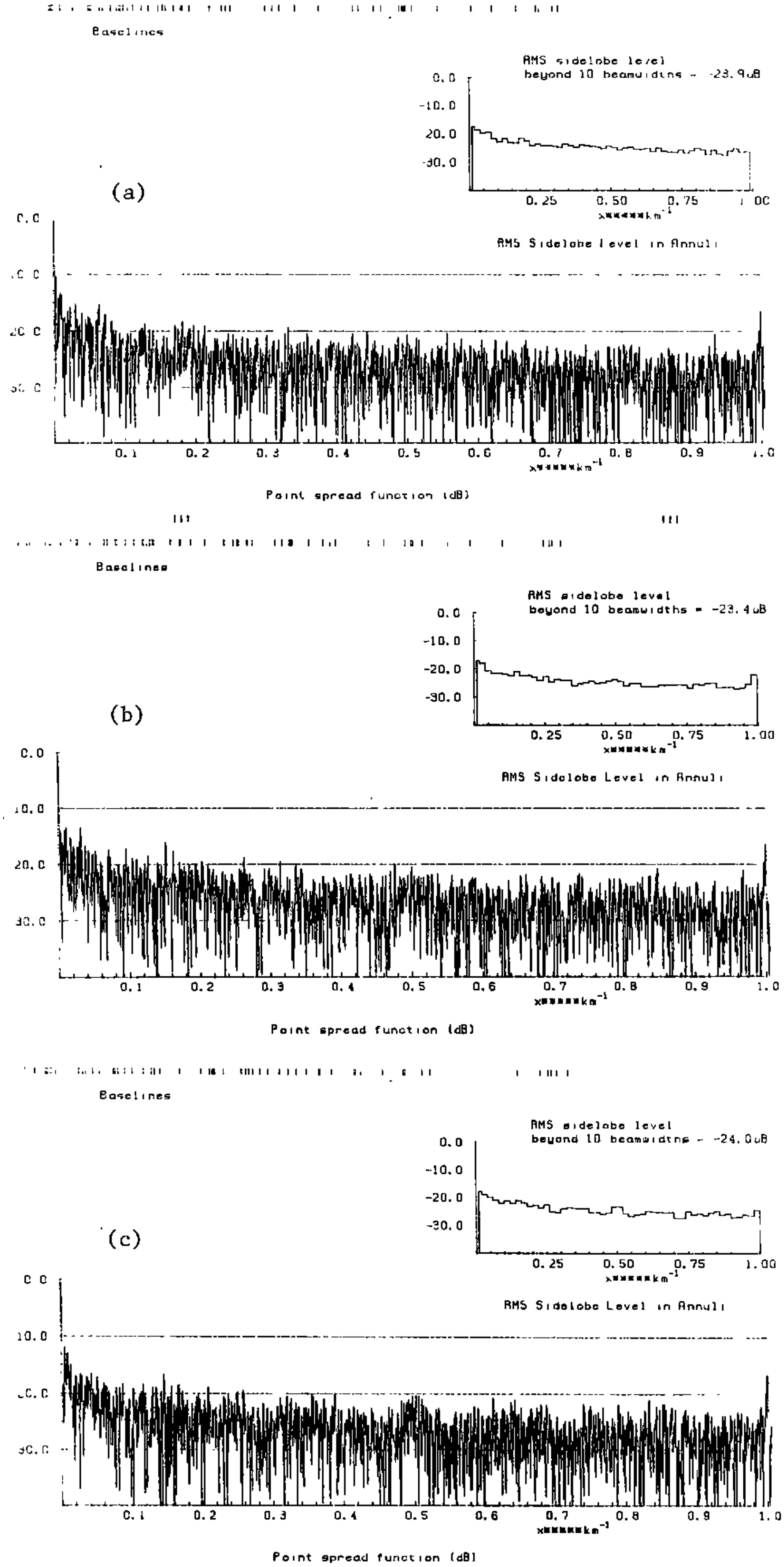

<u>Fig 4.5</u> : Synthesized beam patterns for individual 4-day segments of the 6km minimum redundancy array. (a) days 1-4; (b) days 5-8; (c) days 9-12.

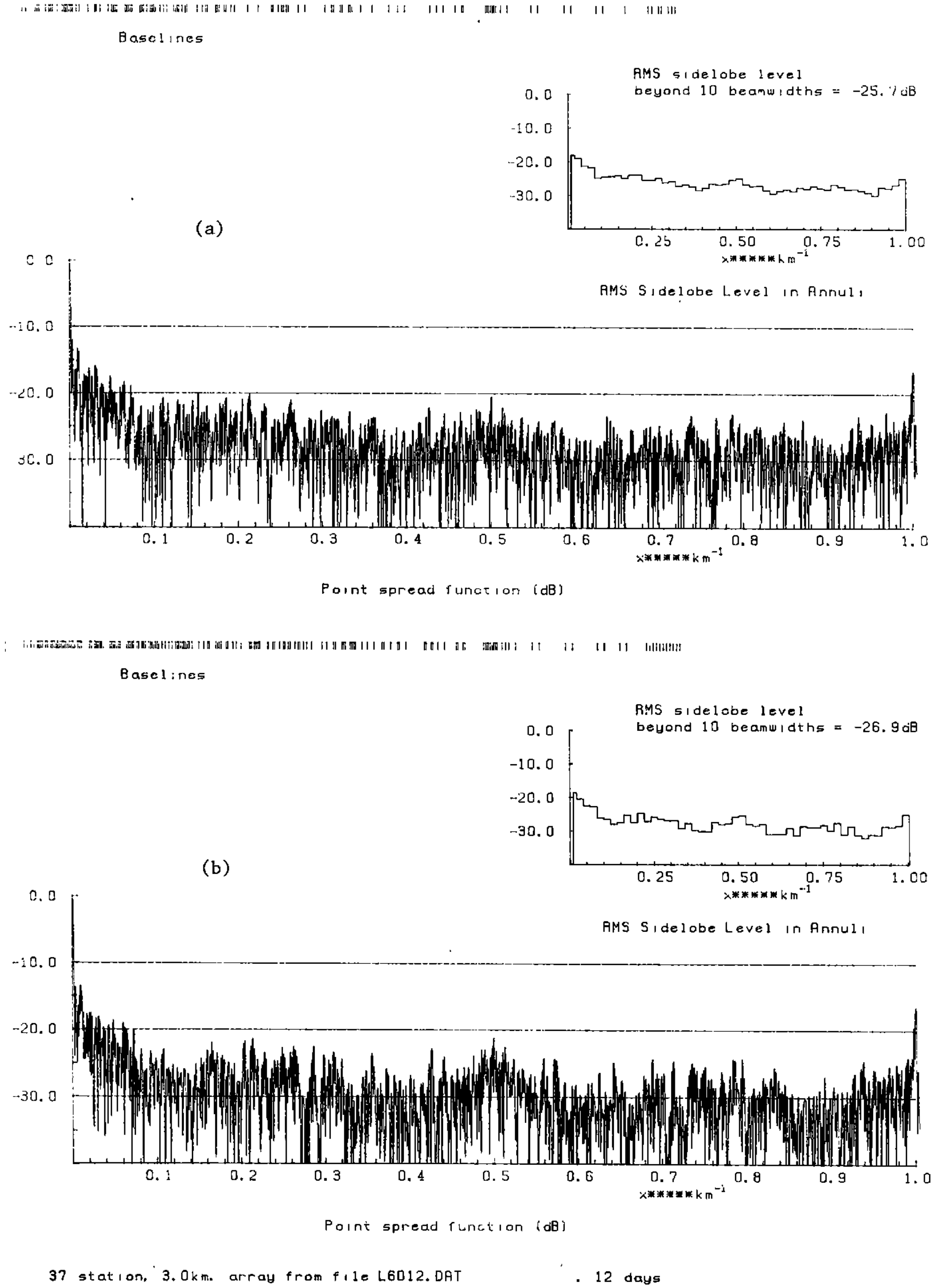

Fig 4.6 : Synthesized beam patterns for longer observations with the 6km minimum redundancy array. (a) days 1-8; (b) days 1-12.

TABLE 4.1

SYNTHESIZED BEAM SIDELOBE LEVELS

Array	Day Range	rms level* (dB)	Peak Level** (dB)
1.5km min.redundancy	1 - 4	-20.7	-15.2
" "	5 - 8	-20.8	-15.2
" "	9 -12	-20.6	-14.7
" "	1 - 8	-23.1	-18.5
" "	1 -12	-25.2	-21.4
3km min.redundancy	1 - 4	-22.3	-15.8
" "	5 - 8	-22.2	-15.0
" "	9 -12	-22.0	-14.7
" "	13-16	-22.3	-15.3
" "	17-20	-21.2	-15.5
" "	21-25	-22.9	-15.4
" "	1 - 8	-24.3	-16.5
" "	1 -12	-25.7	-18.0
" "	1 -16	-27.5	-19.4
" "	1 -20	-29.2	-20.7
" "	1 -24	-31.3	-21.3
" "	1 -25	-32.5	-21.3
6km min.redundancy	1 - 4	-23.9	-15.2
" "	5 - 8	-23.4	-13.2
" "	9 -12	-24.0	-16.3
" "	1 - 8	-25.7	-15.9
" "	1 -12	-26.9	-17.5

* Averaged over the region from 10 beamwidths to the grating ring radius minus 10 beamwidths

**In the region from 20 beamwidths to the grating ring radius minus 20 beamwidths

5.0 SIMULATED OBSERVATIONS

The synthesized beam cross sections presented in the previous section give some idea of the performance of the compact array in its various configurations. However such plots can be misleading, especially when dealing with complex and extended sources. Furthermore, powerful techniques of image restoration such as CLEAN and Maximum Entropy Method (MEM) are now available and it is important to see how well these work on incompletely sampled visibility data. For these reasons a computer simulation of the array has been developed to allow investigation of the array performance when mapping various types of source. The program has the facility of injecting various types of system errors. For the simulations shown below however, only system noise has been added. The assumed frequency is 1.4 GHz, observed bandwidth 16 MHz, source declination -50 deg, and a full 12-hour coverage per day with integration time of 1.2 minutes is assumed. A Kaiser-Bessel convolution function (Schwab, VLA Sci.Mem. No. 129, 1978) was used when gridding the visibilities and uniform weighting (that is, accumulated visibilities were divided by the number of observations falling within that cell - see "Synthesis Mapping", Proceedings of the NRAO-VLA Workshop, June 1982, p.2-13). Dirty maps were cleaned using either CLEAN or MEM; before cleaning they were divided by the transform of the convolution function. For simulations with the 1.5,3 and 6km arrays, the test sources and pixel sizes were scaled so that the ratio of the synthesized beamwidth to source scale and map size remained constant.

5.1 Test Source SPIRAL

The sky distribution for the test source SPIRAL is shown in Fig. 5.1. SPIRAL consists of a sequence of 24 circular gaussian components decreasing in intensity in 1.5 dB steps with a total flux density of 3.4 Jy. The components are resolved by the synthesized beam (full width at half-power = 38" arc compared to a synthesized beamwidth at half-power of 12" arc for the 3km array). Fig. 5.2(a) shows the dirty map (convolution-corrected) resulting from a 4-day observation with the 1.5km array (the first 4 days from Fig. 3.1). Strong positive and negative ring structures resulting from pseudo-grating responses surround and overlap the source so that only the first two or three components are recognizable. The dynamic range of this map, defined by

$$D = -10 \log (3\sigma/M)$$

where σ is the rms fluctuation in source-free regions of the map and M is the map maximum, is 13.4 dB. A related quantity, the map *fidelity*, can be defined by the above equation with σ equal to the rms fluctuation in difference between the map and sky distributions, computed over the region where the sky brightness exceeds 0.1% of its peak value. Before the difference is taken the map is effectively scaled so as to minimize σ. For the map shown in Fig. 5.2(a), the fidelity is 8.3 dB.

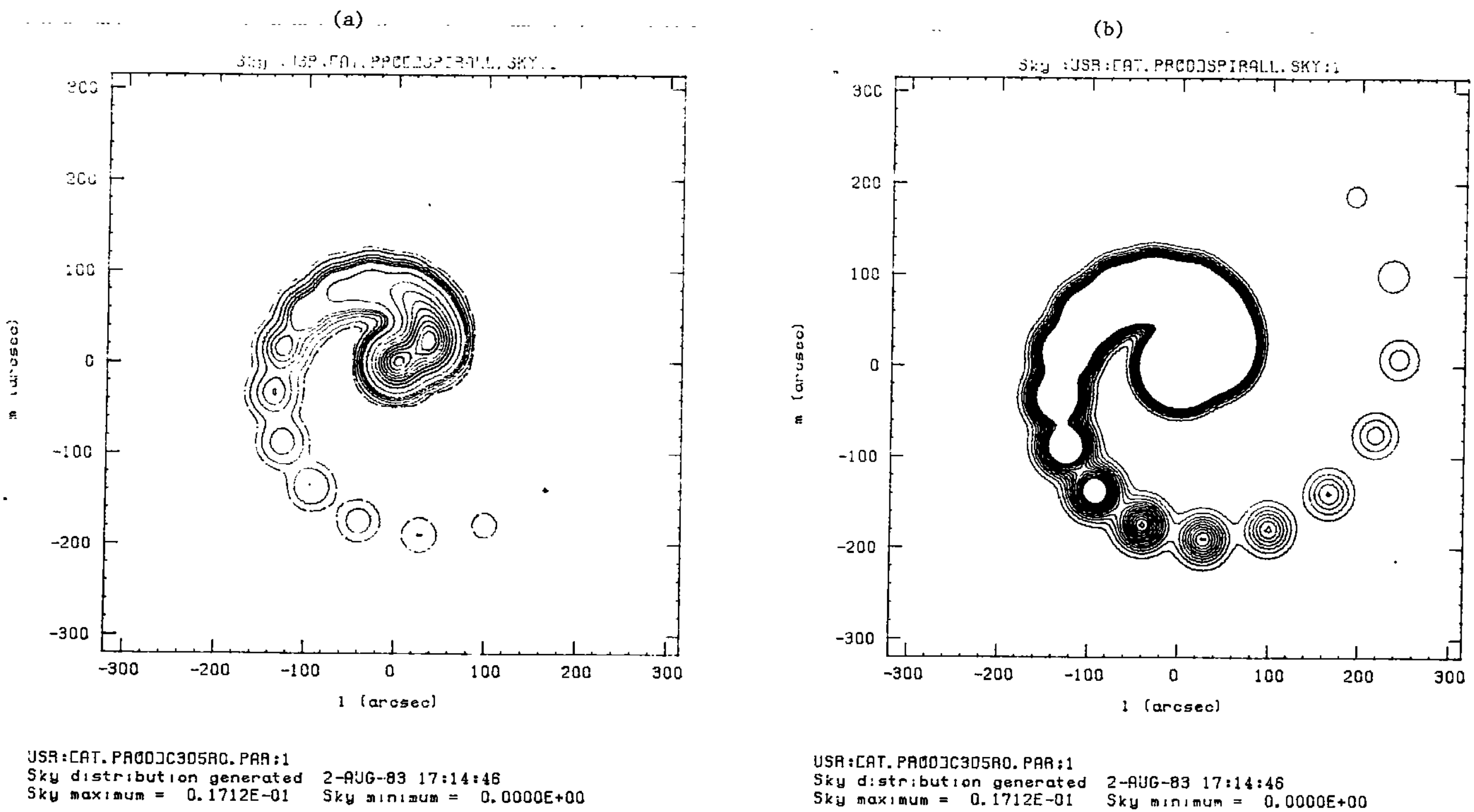

Fig. 5.1 : (a) Sky distribution for the test source SPIRAL, scaled for the 3km array. Only the central quarter of the mapped field is shown. Contour intervals are 0.5% (dashed), 1%,2%,3%,4%,5%,10%,20%,30%,40%,50%,60%,70%,80% and 90% (full lines) of the map maximum. The pixel size is 5" arc in each coordiate. (b) SPIRAL plotted with contours at intervals of 0.1% from 0.1 to 1.5% of the map maximum.

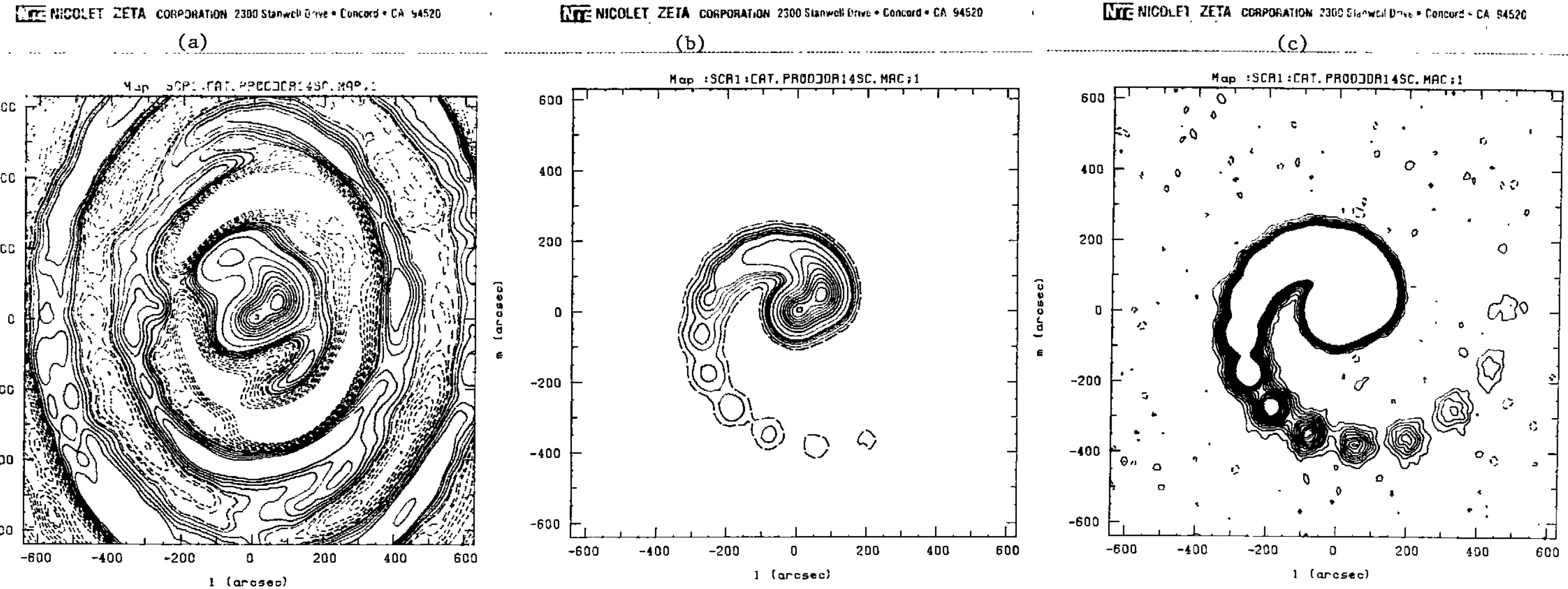

USR:CAT.PROD3SPIRALL1.PAR;1
Array generated 6-FEB-84 17:11:52
USR:CAT.PROD3DR104.ARR;2
Sky distribution generated 6-FEB-84 17:19:00
USR:CAT.PROD3SPIRALL1.SKY;1
Map generated 6-FEB-84 23:06:18
Ha= -6.00 6.00, ha step= 0.02, dec= -50.00, elev lim= 10.
Freq= 1.4 GHz, bandwidth= 16.0 MHz, nch= 1
Pixel= 10.000 sec. Noise & errors added
Day range for synthesis is 1 to 4
Uniform weighting.
Kaiser-Bessel convolution function
Map max= 0.1323E-01 min= -0.1845E-02 rms= 0.5713E-03
Convolution correction applied
Fidelity (to 0.10%) (dB): 8.3 Dynamic Range (dB): 13.4

USR:CAT.PROD3SPIRALL1.PAR;1
Array generated 6-FEB-84 17:11:52
USR:CAT.PROD3DR104.ARR;2
Sky distribution generated 6-FEB-84 17:19:00
USR:CAT.PROD3SPIRALL1.SKY;1
CLEAN restoration, Iter = 9000
Map max = 0.2007E-01 min = -0.4042E-04
Map generated 8-FEB-84 02:06:05
Fidelity (to 0.10%) (dB): 16.0 Dynamic Range (dB): 29.4

USR:CAT.PROD3SPIRALL1.PAR;1
Array generated 6-FEB-84 17:11:52
USR:CAT.PROD3DR104.ARR;2
Sky distribution generated 6-FEB-84 17:19:00
USR:CAT.PROD3SPIRALL1.SKY;1
CLEAN restoration, Iter = 9000
Map max = 0.2007E-01 min = -0.4042E-04
Map generated 8-FEB-84 02:06:05
Fidelity (to 0.10%) (dB): 16.0 Dynamic Range (dB): 29.4

Fig. 5.2 : Dirty map resulting from a 4-day synthesis of the source SPIRAL (Fig. 5.1) using the 1.5km array. Only the central quarter of the mapped area is shown. Contour levels are -10%,-5%,-4%,-3%,-2% and -1% (short dashes), -0.5% and 0.5% (long dashes) and as in Fig. 5.1(a) for positive contours from 1% to 90%. (b) A CLEANed version of the image of Fig. 5.2(a) plotted with the same contour intervals. (c) The CLEANed image plotted with 0.1% contours from -0.6% to -0.1% (dashed) and positive contours, as in Fig. 5.1(b).

Fig. 5.2(b) and (c) show the results of CLEANing the image in Fig. 5.2(a); a total of 9000 CLEAN components were removed from the dirty map and restored using a gaussian beam of half-power widths equal to those of the dirty beam. The improvement is remarkable showing that astrophysically significant results can be anticipated from 4-day syntheses. For the CLEANed map the dynamic range is 29.4 dB and the fidelity 16.0 dB.

Dirty and CLEANed maps resulting from a 4-day synthesis with the 3km array (days 1-4 from Fig. 3.3) are shown in Fig. 5.3. The dirty map is similar in character to that for the 1.5km array [Fig. 5.2(a)] but differs in detail owing to the different sidelobe structure. The CLEANed maps (again 9000 components) are also similar although perhaps slightly inferior with one less source component being clearly defined. Dynamic ranges for the dirty and CLEANed maps respectively are 10.3 and 28.7 dB, somewhat lower than the corresponding figures for the 1.5km maps. Fidelities are 7.0 and 16.5 dB respectively, comparable to those for the 1.5km maps.

The other 4-day sequences produce maps of comparable quality. For this particular source, the 5-8 day sequence produces a slightly better map. Differences such as this result from a better matching of the sampled visibilities to the visibility distribution for the particular source; in general they will not be significant in practice.

Similar maps for a 4-day synthesis with the 6km array are shown in Fig. 5.4. The dirty map is markedly superior to the 1.5 and 3km maps with lower sidelobe levels and more of the source structure visible. This improvement, which is reflected in the dynamic range and fidelity paramaters, 13.1 and 13.5 dB respectively, results from the participation of the extra (6km) antenna and the consequent 50% increase in the number of observed baselines (60 in total compared with 40 for the 1.5 and 3km 4-day arrays). The CLEANed maps, (again 9000 CLEAN components), are also superior with two or perhaps even three additional source components visible. The dynamic range is higher at 29.9 dB but the map fidelity is actually slightly less at 15.8 dB. The map fidelity is limited by a slight smoothing of the image which is inherent in the CLEAN procedure. Because of this, improvements in the weaker parts of the image are not reflected in an improved fidelity.

The performance of the array as a function of the number of days of observaton is clearly of interest. In Fig. 5.5 we show the dynamic range, fidelity and number of clearly visible weak components as a function of number of days of obervaton for CLEANed images of the SPIRAL source from the 3km array. All maps were uniformly weighted and 9000 CLEAN components were subtracted in each case. Even for a (non-optimized) one-day map a dynamic range of over 25 dB is achievable. However improvement is relatively rapid until four days. Beyond this there is a steady improvement in both

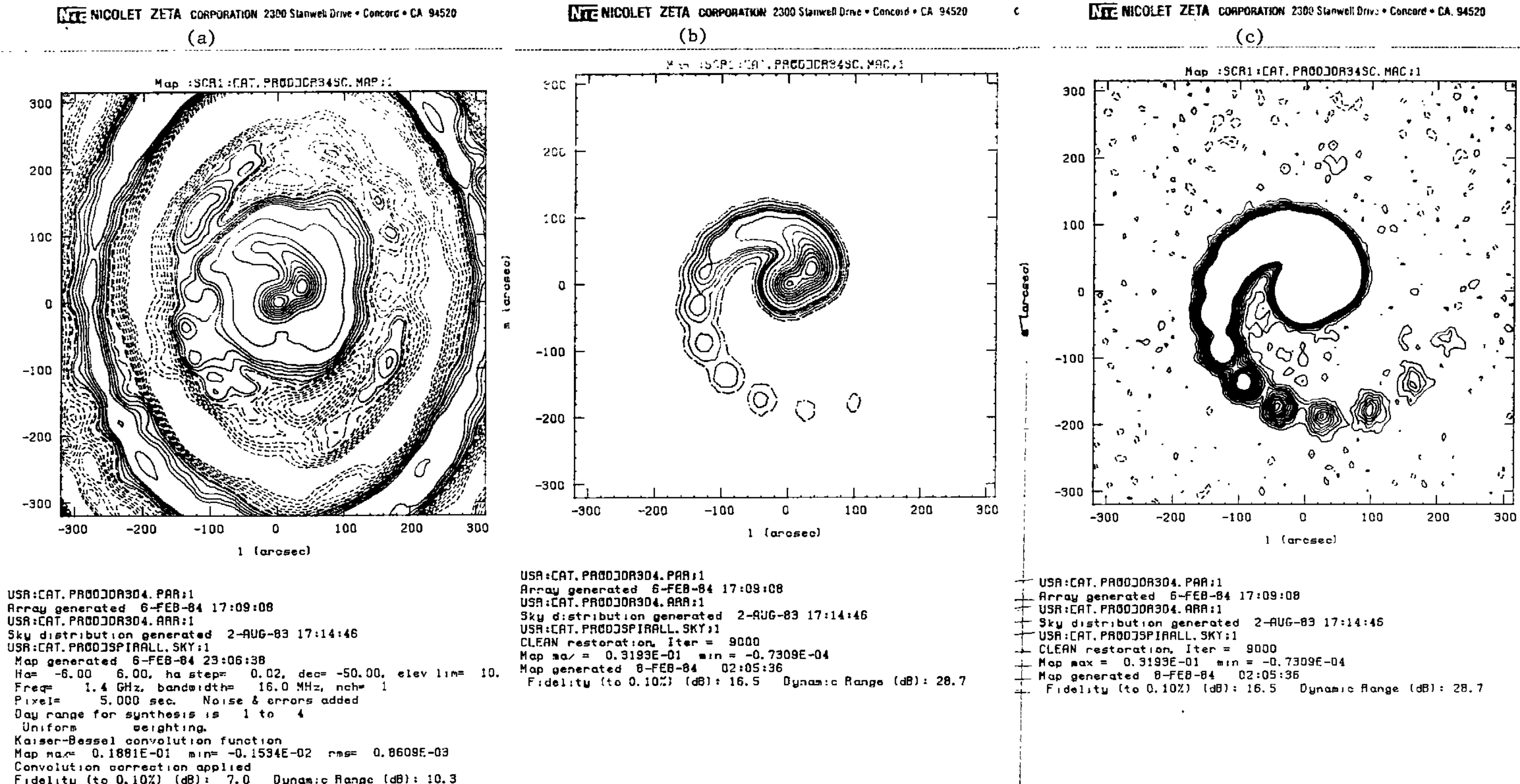

<u>Fig. 5.3</u> : (a) Dirty map resulting from a 4-day synthesis of the source SPIRAL (Fig. 5.1) using the 3km minimum redundancy array. Contour intervals are as in Fig. 5.2(a). (b) and (c) CLEANed versions of the dirty map shown in Fig. 5.3(a). Contour intervals are as in Figs. 5.1(b) and (c) respectively.

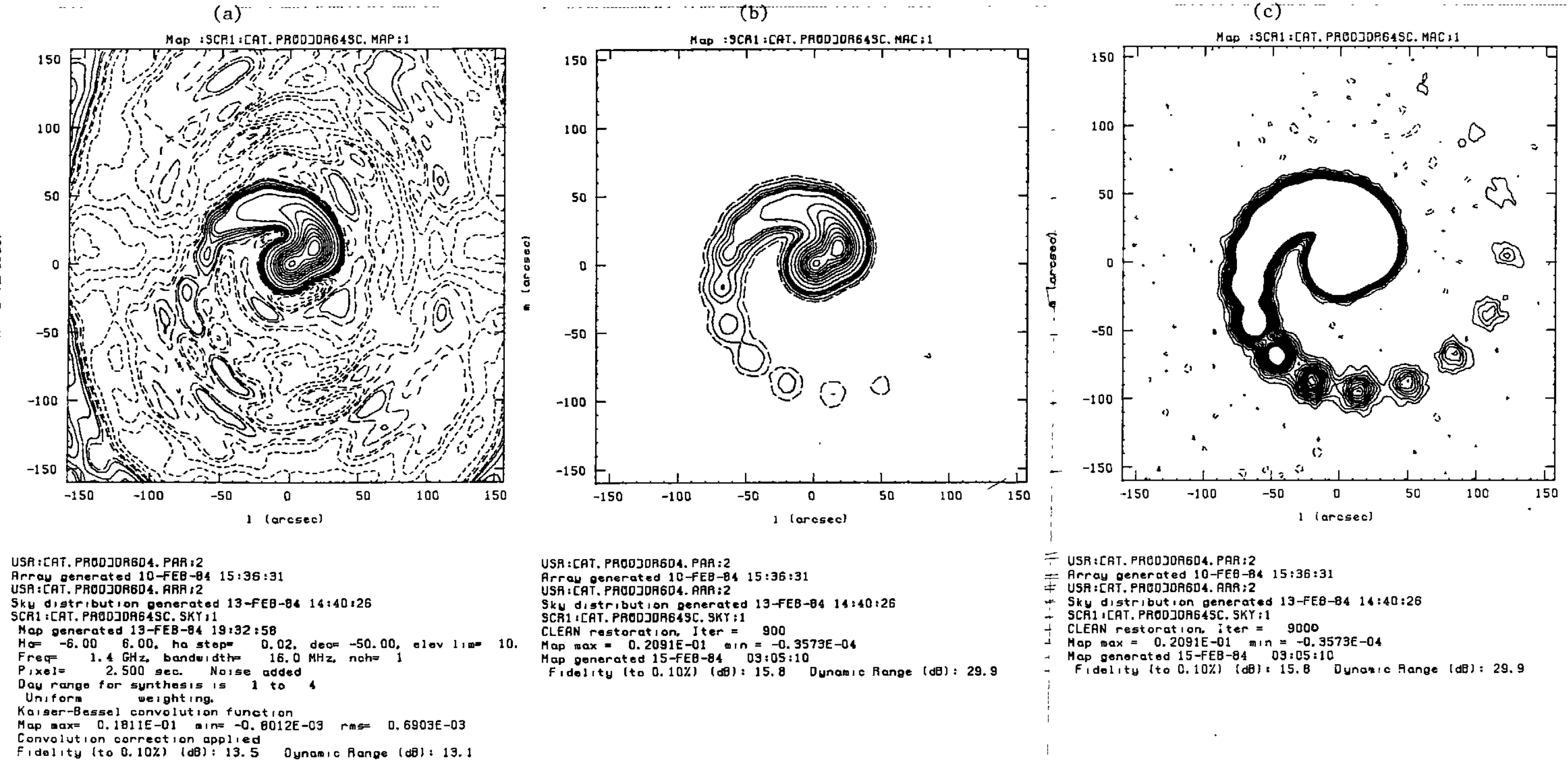

<u>Fig. 5.4</u> : (a) Dirty map resulting from a 4-day synthesis of the source SPIRAL (Fig. 5.1) using the 6km minimum redundancy array. Contour intervals are as in Fig. 5.2(a). (b) and (c) CLEANed versions of the dirty map shown in Fig. 5.4(a). Contour intervals are as in Figs. 5.2(b) and (c) respectively.

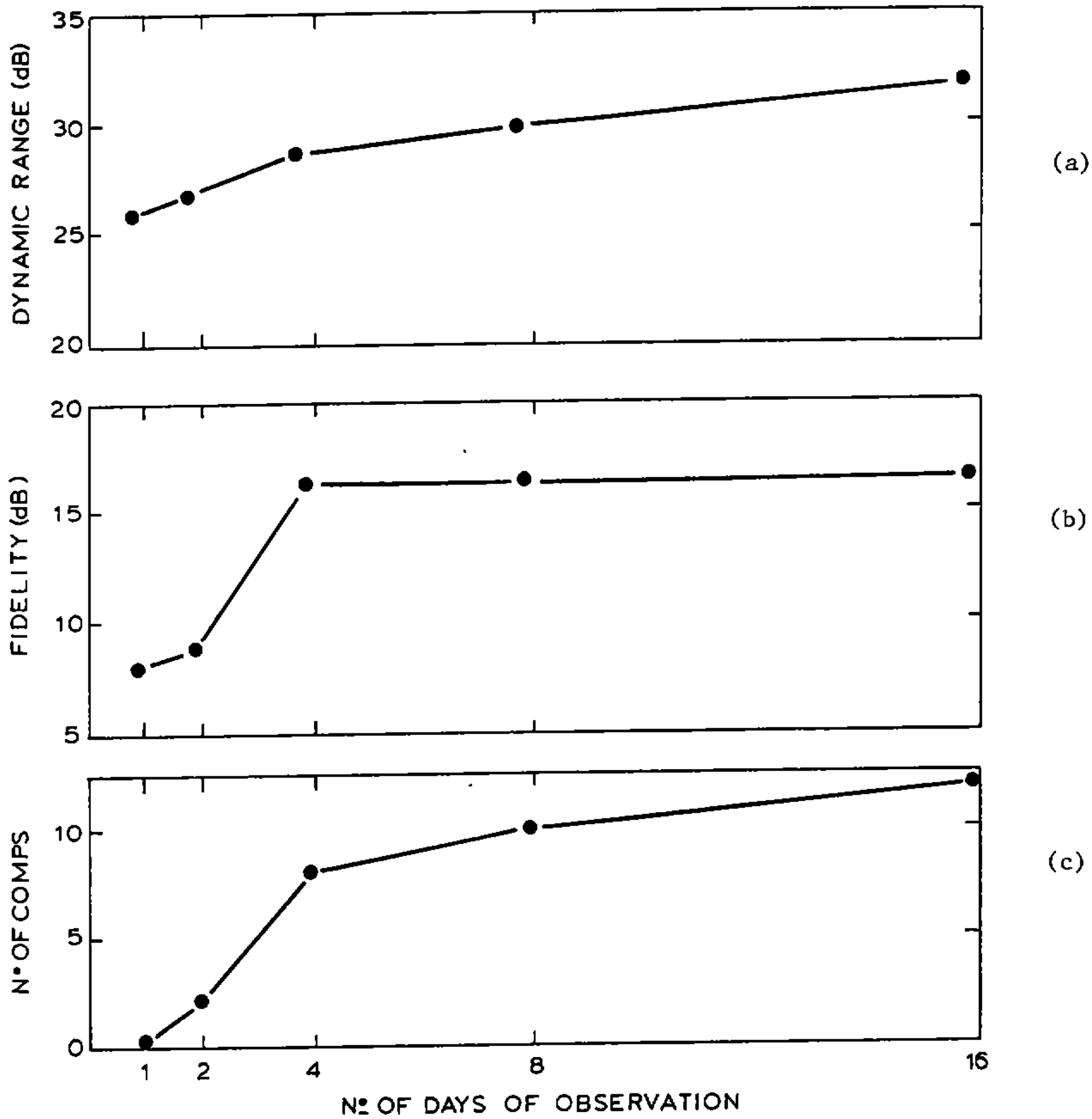

Fig. 5.5 : Dynamic range, map fidelity (see text for definition) and number of clearly identifiable weak components in CLEANed images of SPIRAL as a function of number of days of observaton with the 3km array. The source components were counted from the one at $(\ell,m)=(-140,-40)$. (See Fig. 5.1.)

dynamic range and number of identifiable source components. The fidelity reaches a plateau at 4 days for the reasons stated above.

This figure indicates that, for many purposes, short observations of four days or even less will be adequate. However, it should be remembered that the SPIRAL sky distribution contains no confusing and/or out-of-field sources. In a real situation longer obervations may be necessary for acceptable maps, particularly if the source of interest is not strong compared to the background sources. Note also that antenna gain and pointing errors were assumed to be zero and that the presence of these would degrade a real map.

5.2 Test source ZYGNUS

In contrast to SPIRAL which consists of circular, just-resolved, components, the test source ZYGNUS is a more extended source with complex structure. ZYGNUS, shown in Fig. 5.6, consists of five extended elliptical gaussian components with an accumulated flux density of 245 Jy plus a total of 49 elliptical gaussian components, each barely resolved in one dimension, giving a total flux density of 282.1 Jy.

Dirty and CLEANed maps for a 4-day synthesis with the 1.5km array are shown in Fig. 5.7. The dirty map shows strong distortion resulting from the pseudo-grating structure in the synthesized beam. Fidelity and dynamic range are both low at 6.7 and 8.7 dB respectively. CLEANing with 9000 components produces a much improved image (fidelity of 12.8 dB and dynamic range of 22.3 dB) but still leaves astrophysically interesting looking artefacts such as the "horns" projecting from the lefthand edge of the source [Fig. 5.7(c)]. It is possible that further CLEANing would improve this image.

Maps resulting from a 4-day synthesis with the 3km array are shown in Fig. 5.8. The dirty map looks a little better than that for the 1.5km array [Fig. 5.7(a)] and in fact has a higher dynamic range, 10.4 dB. The fidelity is slightly lower at 6.3 dB. The CLEANed image is comparable to those for the 1.5km array (fidelity 12.7 dB and dynamic range 22.0 dB) but appears to have less serious artefacts.

The fidelity and dynamic range figures for the CLEANed maps are not as good for ZYGNUS as they are for SPIRAL. This is probably because ZYGNUS is more extended and hence more difficult to CLEAN properly. MEM is more suited to such sources and Fig. 5.9 shows the result of image restoration using the AIPS implementation of MEM. The restored image is clearly much better than that from CLEAN and is in fact very close to the original sky distribution. This is

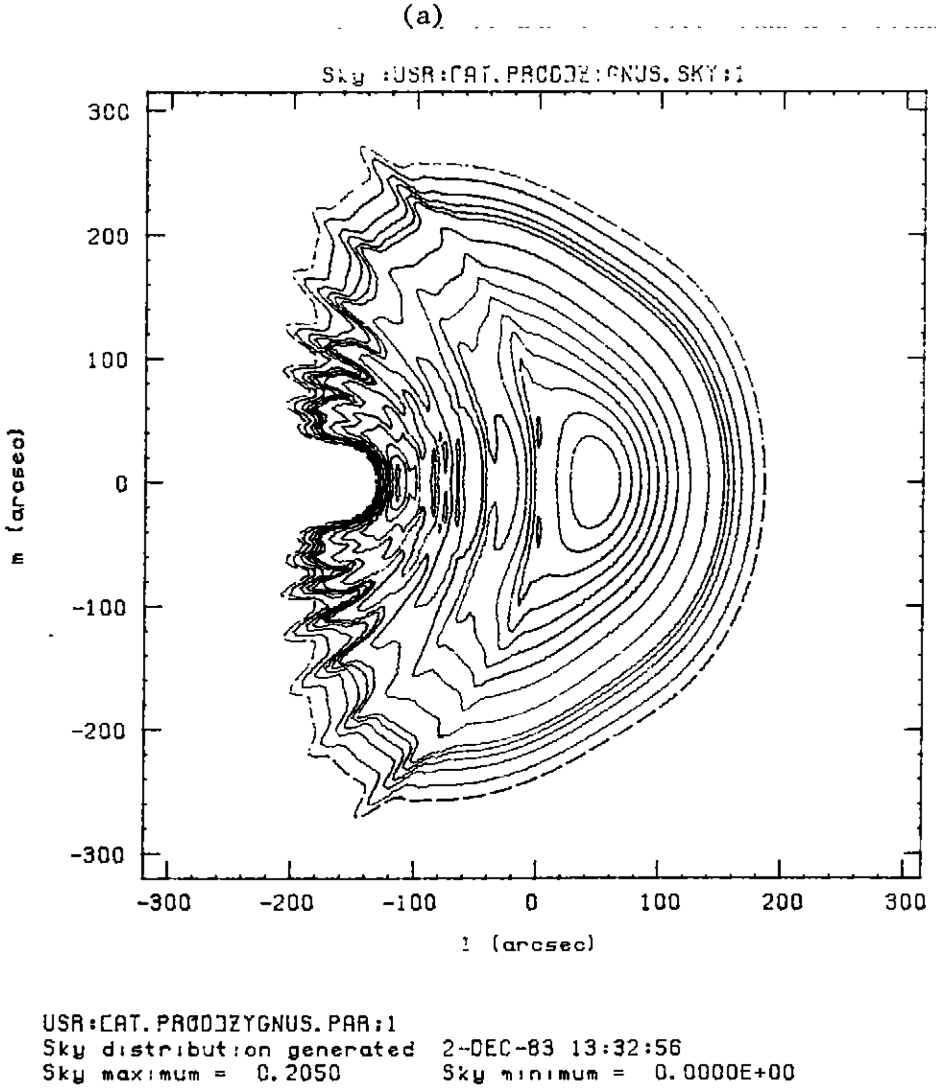

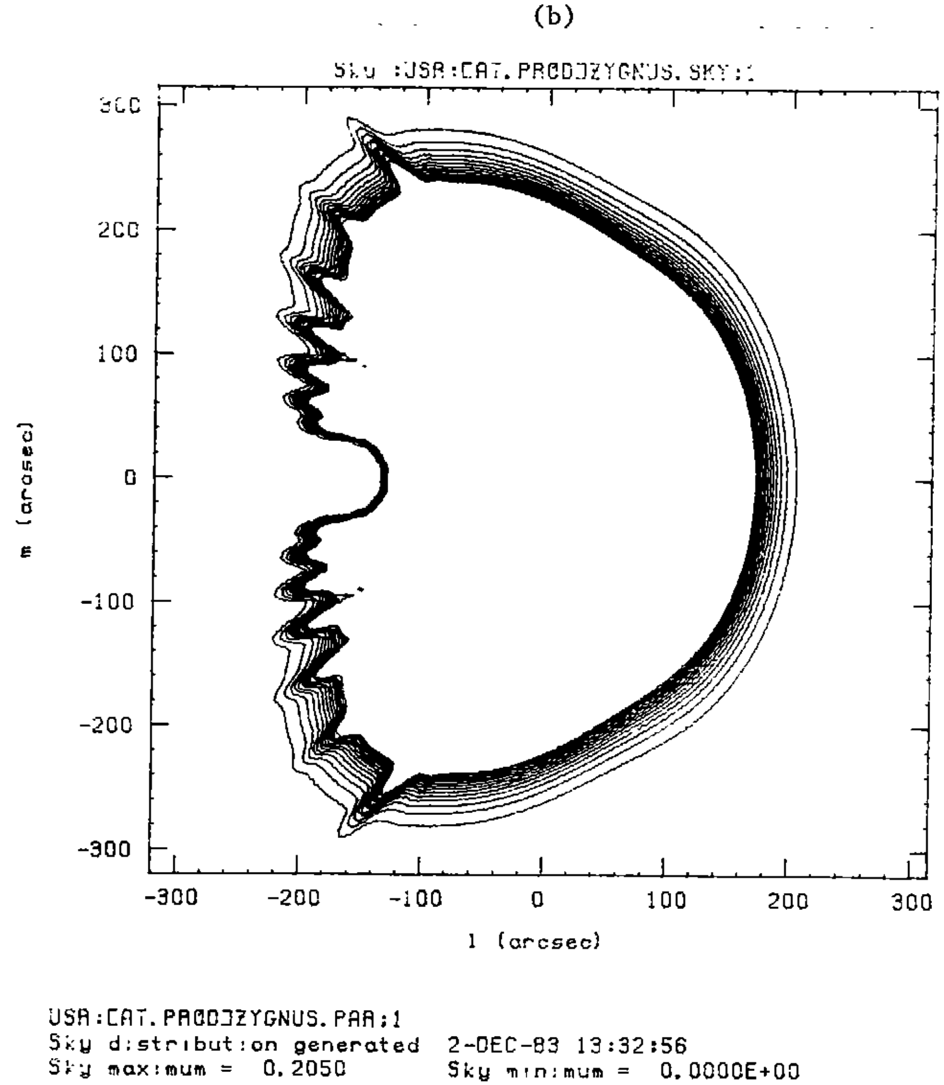

Fig. 5.6 : (a) and (b) Sky distribution for the test source ZYGNUS, scaled for the 3km array. Only the central quarter of the field is shown. Contour intervals are as for fig. 5.1 (a) and (b) respectively.

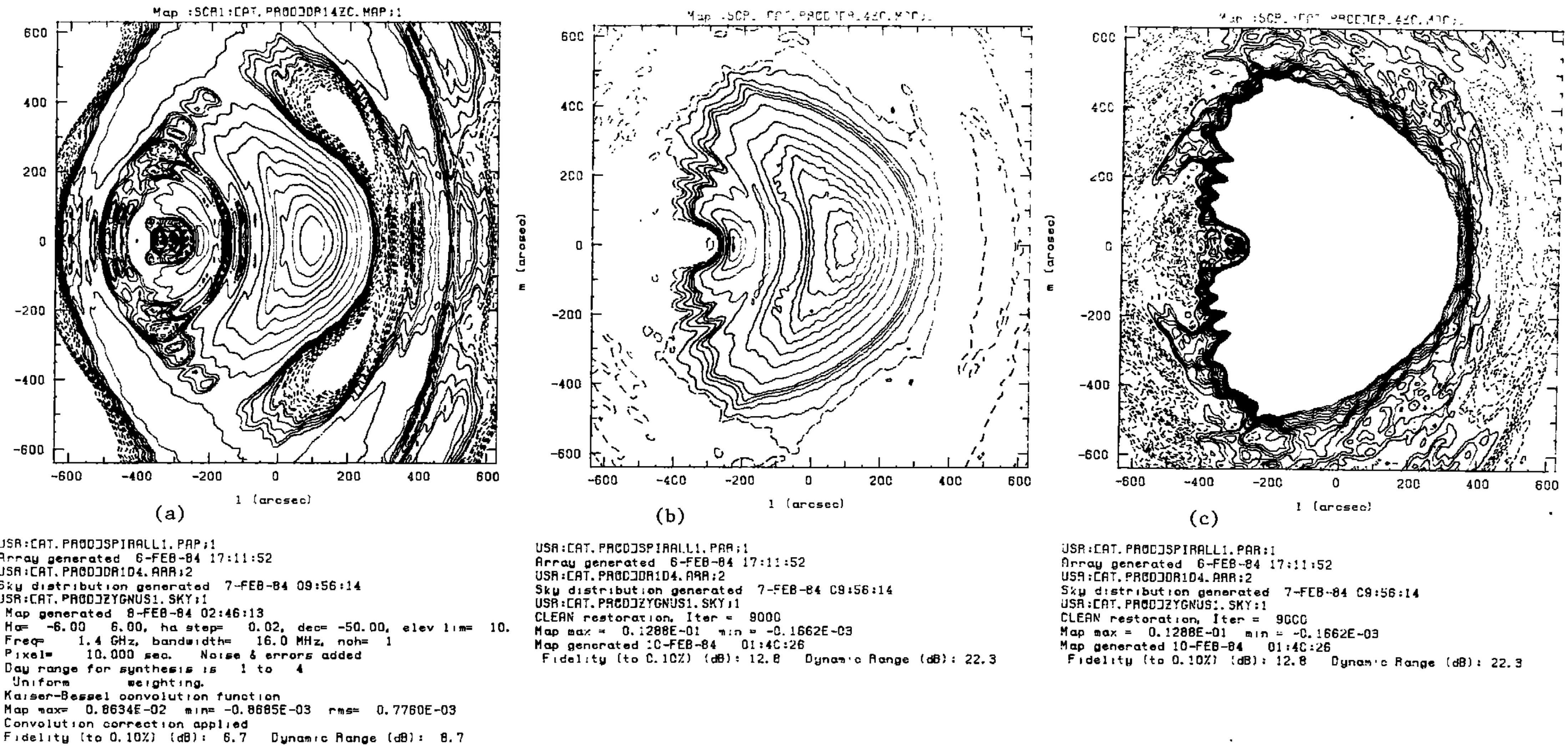

Fig. 5.7 : (a) Dirty map from a 4-day synthesis with the 1.5km array of the source Zygnus. Contour intervals are as for Fig. 5.2(a). (b) and (c) CLEANed versions of the dirty map. Contour intervals are as for Fig. 5.2(b) and (c) respectively.

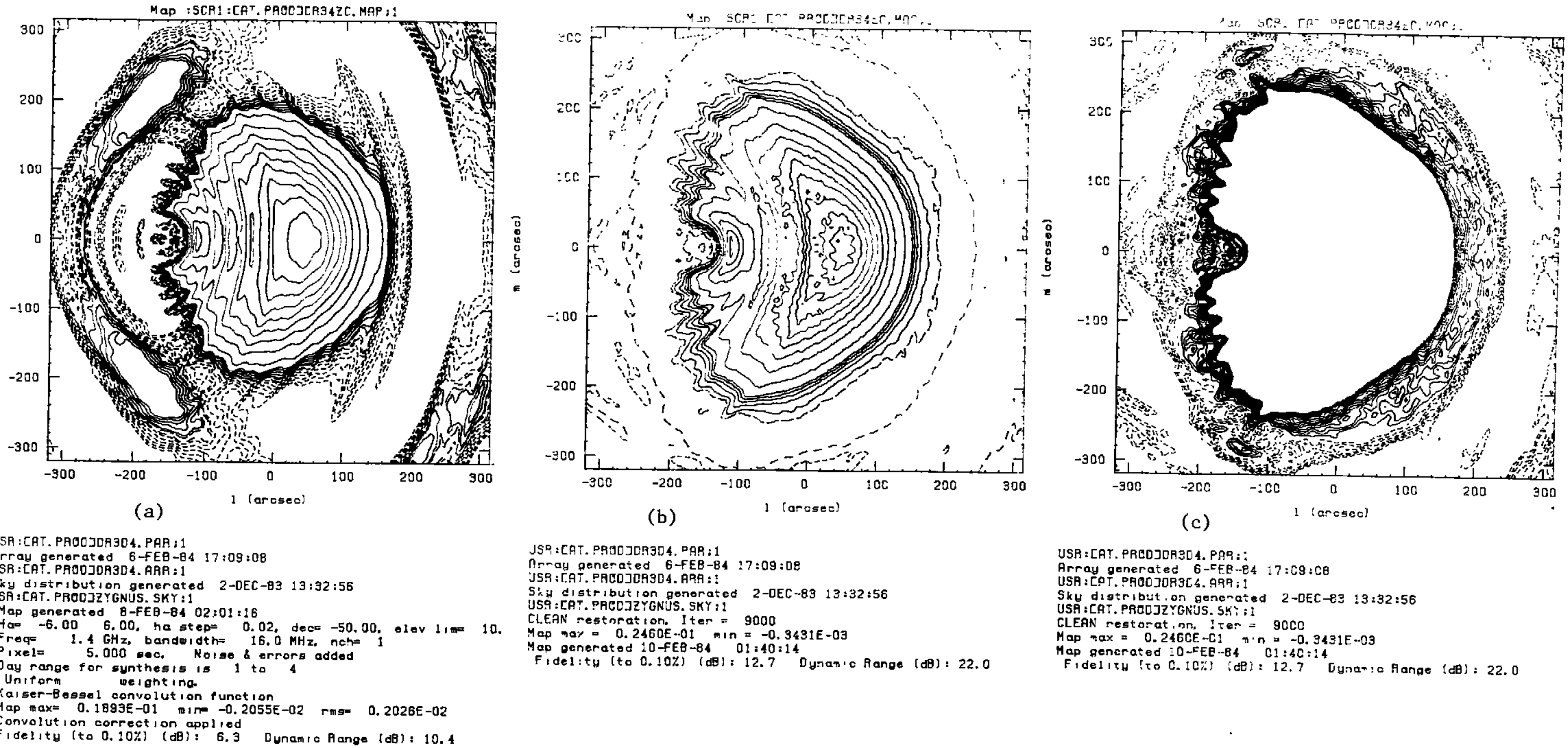

<u>Fig. 5.8</u> : (a) Dirty map from a 4-day synthesis with the 3km array of the source ZYGNUS; Contour levels are as for Fig. 5.2(a). (b) and (c) CLEANed versions of the dirty map shown in Fig. 5.8(a); contour intervals ar as in Fig. 5.2(b) and (c) respectively.

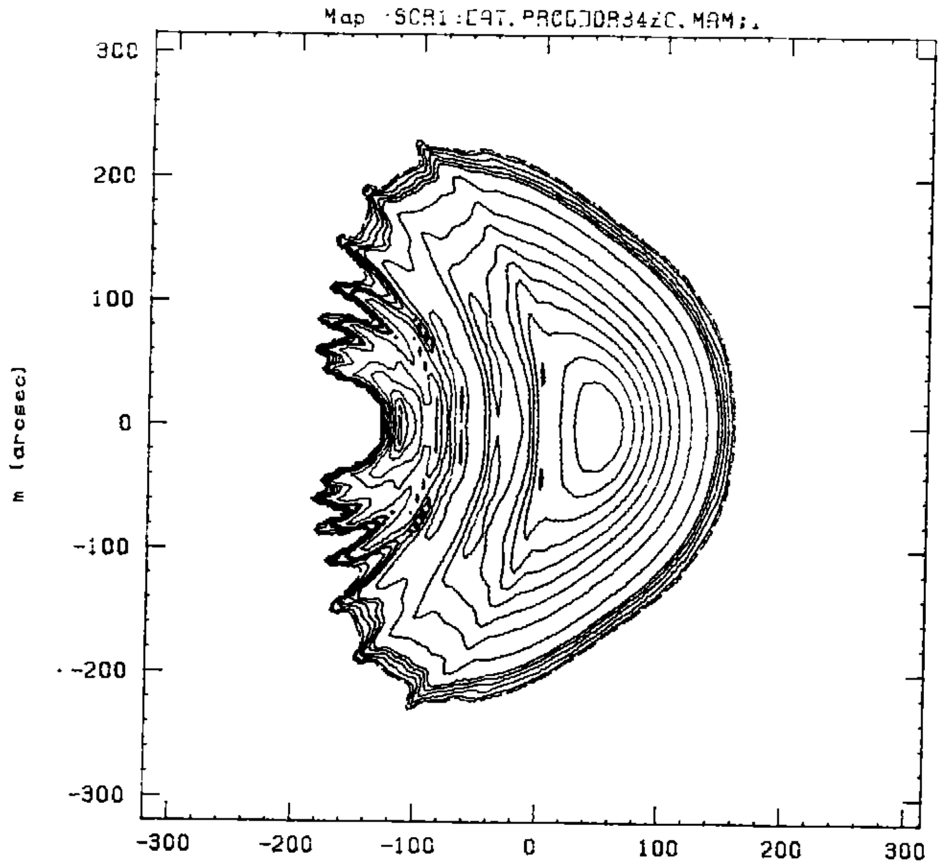

(a)

USR:CAT.PRODJDR3D4.PAR;1
Array generated 6-FEB-84 17:09:08
USR:CAT.PRODJDR3D4.ARR;1
Sky distribution generated 2-DEC-83 13:32:56
USR:CAT.PRODJZYGNUS.SKY;1
Map generated 8-FEB-84 02:01:16
Ha= -6.00 6.00, ha step= 0.02, dec= -50.00, elev lim= 10.00
Freq= 1.4 GHz, bandwidth= 16.0 MHz, nch= 1
Pixel= 5.000 sec. Noise & errors added
Day range for synthesis is 1 to 4
Uniform weighting.
Kaiser-Bessel convolution function
Map max= 0.1893E-01 min= -0.2055E-02 rms= 0.2026E-02
Convolution correction applied

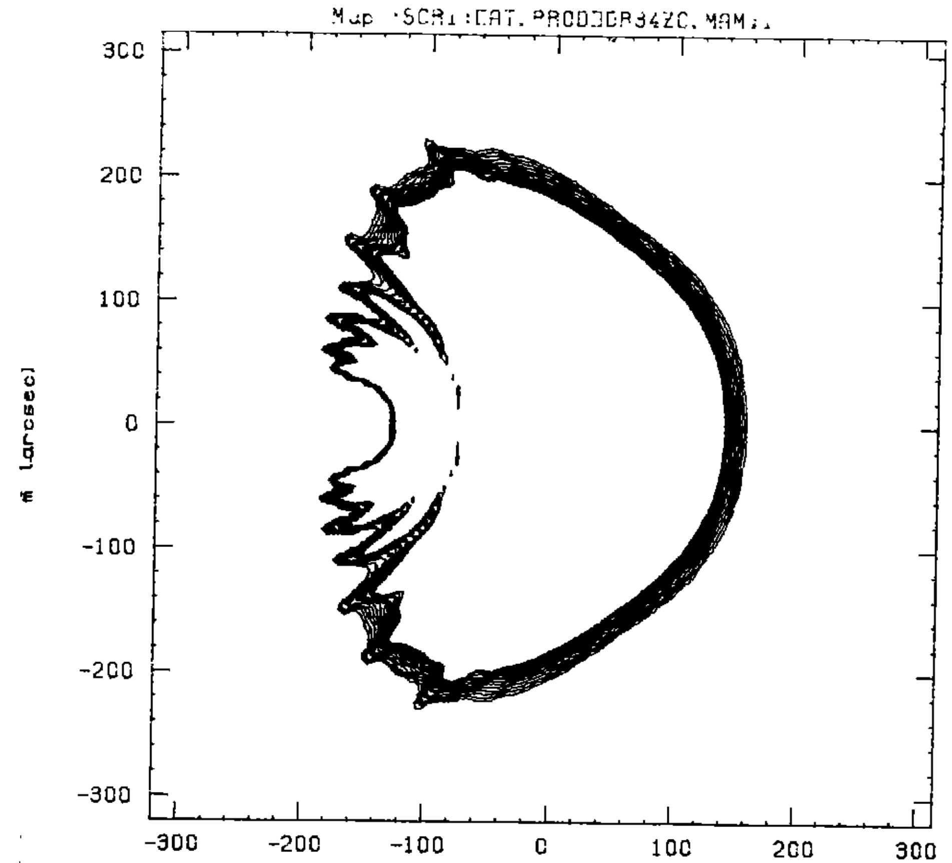

(b)

USR:CAT.PRODJDR3D4.PAR;1
Array generated 6-FEB-84 17:09:08
USR:CAT.PRODJDR3D4.ARR;1
Sky distribution generated 2-DEC-83 13:32:56
USR:CAT.PRODJZYGNUS.SKY;1
Map generated 8-FEB-84 02:01:16
Ha= -6.00 6.00, ha step= 0.02, dec= -50.00, elev lim= 10.00
Freq= 1.4 GHz, bandwidth= 16.0 Mhz, nch= 1
Pixel= 5.000 sec. Noise & errors added
Day range for synthesis is 1 to 4
Uniform weighting.
Kaiser-Bessel convolution function
Map max= 0.1893E-01 min= -0.2055E-02 rms= 0.2026E-02
Convolution correction applied

Fig. 5.9 : (a) and (b) Image of the source Zygnus restored using MEM from the 3km 4-day dirty map shown in Fig. 5.8(a). Contour intervals are as for Fig. 5.2(b) and (c) respectively.

quantified by the high fidelity, 21.2 dB, of the image. (Dynamic range is not meaningful for MEM images since background noise is suppressed.) The main difference between the sky and the restored map is that, at low levels, the source cuts off more sharply in the latter. This is evident in Fig. 5.9(b) and can also be seen in Fig. 5.10. Overall, however, the restoration is excellent. ZYGNUS is of course a strong source and such good results could not be expected on a weaker object of similar complexity.

Fig. 5.11(a) shows the dirty map from a 4-day synthesis with the 6km minimum redundancy array. As for SPIRAL, the 6km array produces a cleaner map in a given time compared with the 1.5 or 3km arrays. The fidelity and dynamic range parameters are 11.2 and 11.3 dB respectively. The CLEANed image, shown in Fig. 5.11(b) and (c) is also better than that for the shorter arrays with fidelity and dynamic range 13.0 and 25.6 dB respectively. This is not surprising, since improved u-v coverage should be more important for a more complex source.

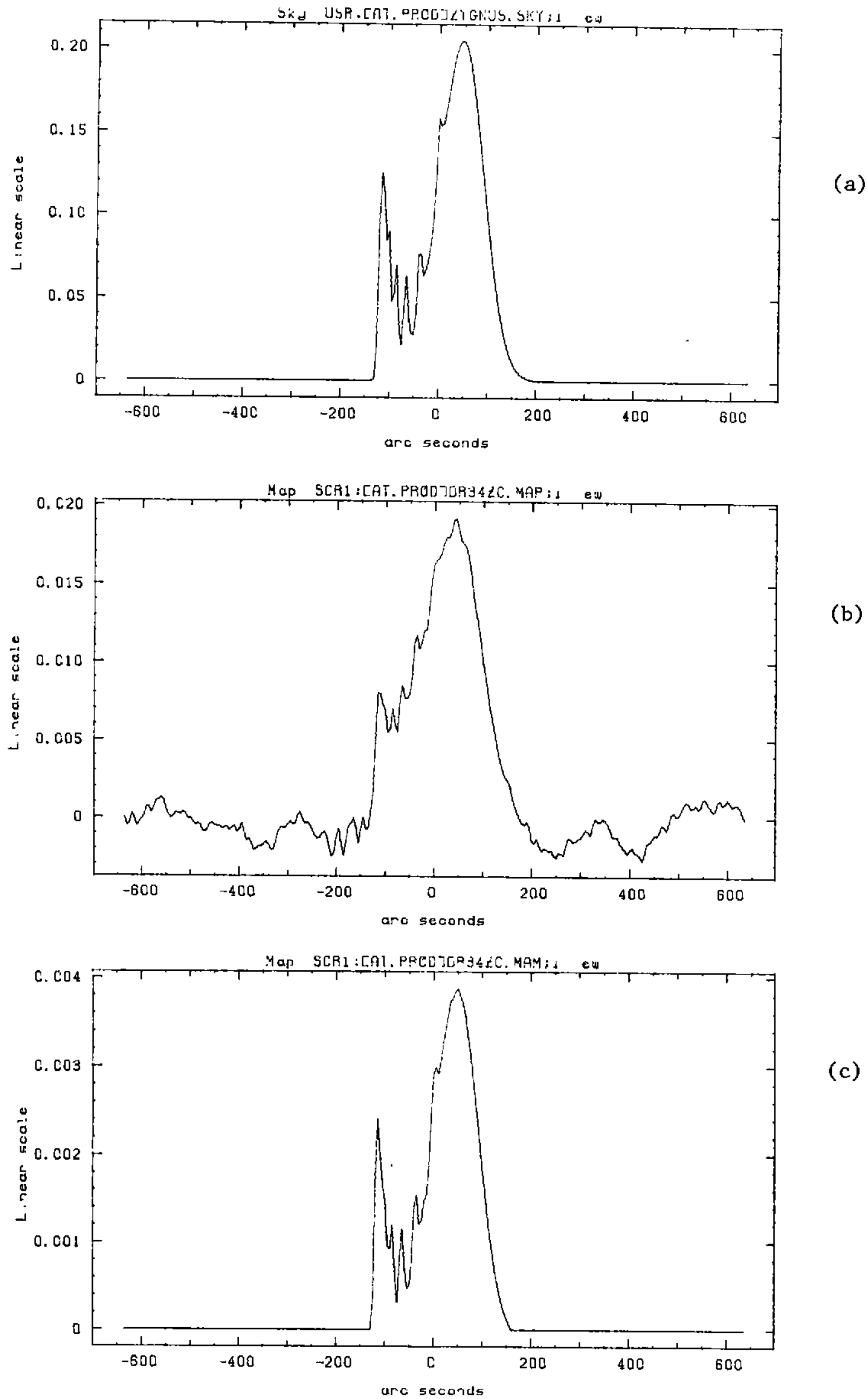

<u>Fig. 5.10</u> : (a) East-west section at β=0 through the sky distribution for test source ZYGNUS. The section extends across the whole field. (b) A similar section through the dirty map, Fig. 5.8(a). (c) A similar section through the MEM-restored image, Fig. 5.9.

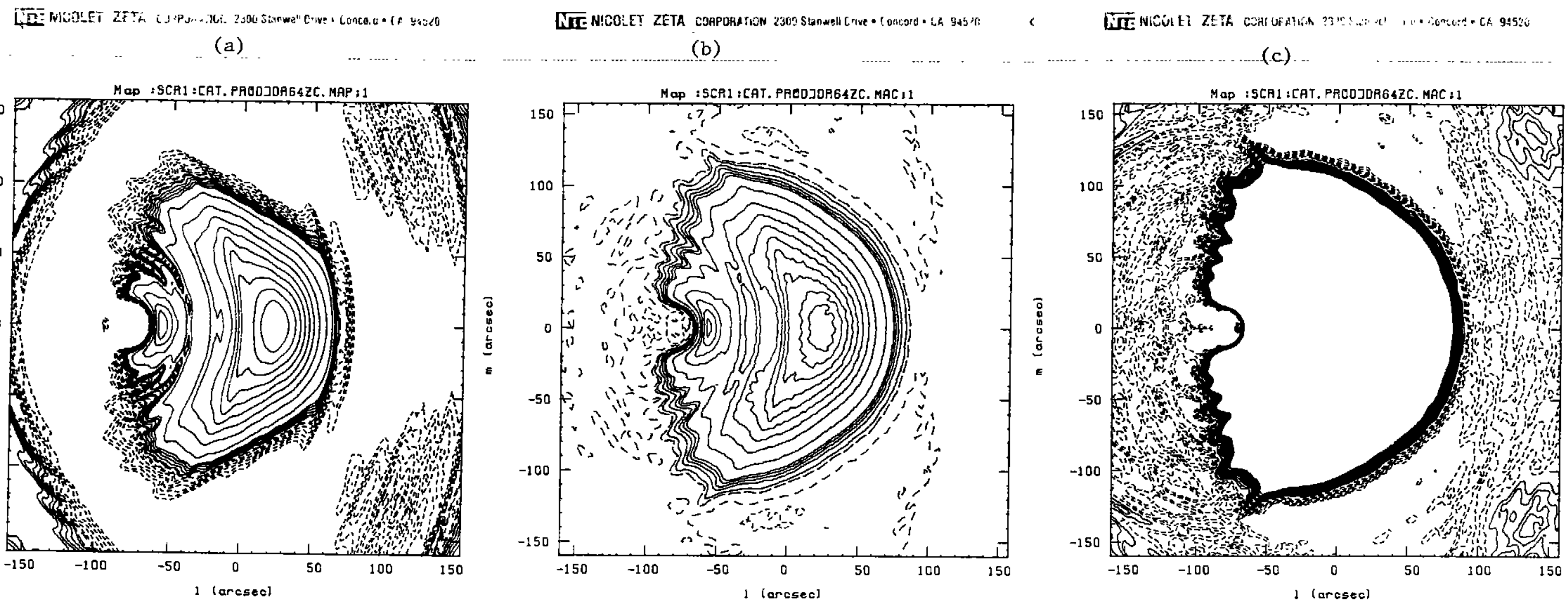

USA:CAT.PRODJDR6D4.PAR;2
Array generated 10-FEB-84 15:36:31
USA:CAT.PRODJDR6D4.ARR;2
Sky distribution generated 14-FEB-84 10:19:24
SCR1:CAT.PRODJDR64ZC.SKY;1
Map generated 14-FEB-84 11:47:50
Ha= -6.00 6.00, ha step= 0.02, dec= -50.00, elev lim= 10.1
Freq= 1.4 GHz, bandwidth= 16.0 MHz, nch= 1
Pixel= 2.500 sec. Noise added
Day range for synthesis is 1 to 4
Uniform weighting.
Kaiser-Bessel convolution function
Map max= 0.4304E-01 min= -0.7714E-02 rms= 0.4042E-02
Convolution correction applied
Fidelity (to 0.10%) (dB): 11.2 Dynamic Range (dB): 11.3

USA:CAT.PRODJDR6D4.PAR;2
Array generated 10-FEB-84 15:36:31
USA:CAT.PRODJDR6D4.ARR;2
Sky distribution generated 14-FEB-84 10:19:24
SCR1:CAT.PRODJDR64ZC.SKY;1
CLEAN restoration, Iter = 9000
Map max = 0.5586E-01 min = -0.1076E-02
Map generated 15-FEB-84 03:25:33
Fidelity (to 0.10%) (dB): 13.0 Dynamic Range (dB): 25.6

USA:CAT.PRODJDR6D4.PAR;2
Array generated 10-FEB-84 15:36:31
USA:CAT.PRODJDR6D4.ARR;2
Sky distribution generated 14-FEB-84 10:19:24
SCR1:CAT.PRODJDR64ZC.SKY;1
CLEAN restoration, Iter = 9000
Map max = 0.5586E-01 min = -0.1076E-02
Map generated 15-FEB-84 03:25:33
Fidelity (to 0.10%) (dB): 13.0 Dynamic Range (dB): 25.6

Fig 5.11 : (a) Dirty map from a 4-day synthesis with the 6km array of the source ZYGNUS; Contour intervals are as for Fig. 5.2(a). (b) and (c) CLEANed versions of the dirty map shown in Fig. 5.11(a); Contour intervals are as for Fig. 5.2(b) and (c) respectively.

6.0 RECOMMENDATIONS FOR FUTURE EXTENSIONS

We believe that the compact array design presented in this document satisfies most requirements within the limitations discussed in the first section. It is clear however, that extensions of the array would be desirable in future. In this section we discuss four possible extensions. Variations of these and different ideas will no doubt surface with the passage of time. It should be noted that we have not considered extension of the Long Baseline Array and its eventual combination with the Compact Array, although these are clearly desirable in the long term. Decisions on priorities for these and other options will have to be made at the appropriate time. However, we should try to anticipate these extensions and as far as possible provide for them, or at least not preclude them, in the current design.

6.1 Two-dimensional Compact Array

For observations at high frequencies (say 22 GHz and above) where northern hemisphere observatories have difficulty observing objects in the southern equatorial zone (say -30 deg to 0 deg declination), a two-dimensional array of dimensions 1.0 to 1.5km would clearly be of great value. The simplest way to achieve this would be to place a N-S spur track of approx. 1 km length either north or south of the E-W track. Such a track would be entirely on CSIRO property.

A preliminary examination of the problem suggests that the intersection point should be near the centre of the track and close to a group of stations, for example, at location 109. This T arrangement has the disadvantage that all baselines from a given antenna on the spur track to antennas on the E-W track have the same N-S baseline component and hence the same "v" on the u-v plane for a given declination. However, given that we have the E-W track, this is difficult to avoid. U-shaped configurations involving two spur tracks can be envisaged, but these would obviously be more expensive.

For observations at 115 GHz, where only the central 10m of the antenna is illuminated, additional stations will probably be required on the E-W track.

6.2 An Extra Station at 6km

With only 35 stations in the 0-3km zone and two stations at 6km, coverage of the 3-6km range of baselines is incomplete and not very uniform. Of the 196 possible baselines, only 57 are observable with the configuration described in Section 3.4. This may be a problem for observations of complex fields. Addition of a third station at location 383, that is, nine increments or 138m from the end of the array would allow observation of 26 extra baselines.

6.3 Additional Antenna(s) on the 0-3km Rail-track

Addition of a sixth antenna on the 0-3km rail-track would increase the speed of the 1.5 and 3km arrays by 50% and increase the number of baselines obtained per day in the 3-6km range by 20%. Even more importantly, it would improve the self-calibration of the arrays significantly. The observing sequences described in Section 3 would have to be altered, but no change in station locations would be required.

6.4 Extension of the Array Length

For observations at relatively low frequencies of, for example, supernova remnants or radio galaxies, improvement of the resolution of the compact array would be of considerable benefit. With only the 0-3km section of rail-track, extension of the array length would require extra groups of stations similar to that at the 6km point at 9km, 12km, 15km, etc. If an extension of this nature were contemplated it might be more cost-effective to extend the continuous rail-track to the 6km point. Then groups of stations would be required at 6km intervals rather than 3km intervals. Any such extension should be closely integrated with the linking of the Compact Array and the Long Baseline Array.

APPENDIX 1.

This appendix lists antenna locations and baselines formed for each day of the various arrays. Baselines marked with an asterisk have been previously observed in this sequence. Stations used for each array are also listed.

A.1 The 1.5km minimum redundancy array

Day	Antenna Locations					Baselines									
1	109	111	148	163	182	2	15	19	34	37	39	52	54	71	73
2	100	110	163	168	189	5	10	21	26	53	58	63	68	79	89
3	98	113	173	182	189	7	9	15*	16	60	69	75	76	84	91
4	100	129	147	190	196	6	18	29	43	47	49	61	67	90	96
5	102	140	147	182	195	7*	13	35	38	42	45	48	55	80	93
6	109	113	140	173	190	4	17	27	31	33	50	60*	64	77	81
7	98	102	128	168	190	4*	22	26*	30	40	62	66	70	88	92
8	98	102	110	172	196	4*	8	12	24	62*	70*	74	86	94	98
9	98	109	112	163	195	3	11	14	32	51	54*	65	83	86*	97
10	100	113	128	172	195	13*	15*	23	28	44	59	67*	72	82	95
11	102	111	148	168	189	9*	20	21*	37*	41	46	57	66*	78	87
12	111	140	147	172	196	7*	24*	25	29*	32*	36	49*	56	61*	85

Stations used :
98 100 102 109 110 111 112 113 128 129 140 147 148 163 168 172 173 182 189 190 195 196

A.2 The 3km minimum redundancy array

Day	Antenna Locations					Baselines									
1	0	12	64	190	195	5	12	52	64	126	131	178	183	190	195
2	0	10	84	189	196	7	10	74	84	105	112	179	186	189	196
3	8	12	102	147	168	4	21	45	66	90	94	135	139	156	160
4	0	32	110	148	168	20	32	38	58	78	110	116	136	148	168
5	2	6	110	140	172	4*	30	32*	62	104	108	134	138	166	170
6	14	45	113	128	168	15	31	40	55	68	83	99	114	123	154
7	2	45	102	148	189	41	43	46	57	87	100	103	144	146	187
8	14	32	109	172	195	18	23	63	77	86	95	140	158	163	181
9	14	84	163	182	190	8	19	27	70	79	98	106	149	168*	176
10	8	113	128	163	172	9	15*	35	44	50	59	105*	120	155	164
11	0	10	129	140	182	10*	11	42	53	119	129	130	140*	172	182
12	2	4	84	173	195	2	22	80	82	89	111	169	171	191	193
13	2	8	64	182	196	6	14	56	62*	118	132	174	180	188	194
14	6	45	147	173	190	17	26	39	43*	102	128	141	145	167	184
15	16	64	140	173	189	16	33	48	49	76	109	124	125	157	173
16	12	100	129	173	189	16*	29	44*	60	73	88	89*	117	161	177
17	45	110	148	182	195	13	34	38*	47	65	72	85	103*	137	150
18	10	102	111	148	172	9*	24	37	46*	61	70*	92	101	138*	162
19	4	32	111	147	189	28	36	42*	78*	79*	107	115	143	157*	185
20	12	16	109	112	163	3	4*	51	54	93	96	97	100*	147	151
21	14	98	147	173	189	16*	26*	42*	49*	75	84*	91	133	159	175
22	6	8	128	148	173	2*	20*	25	45*	120*	122	140*	142	165	167*
23	4	16	129	168	196	12*	28*	39*	67	113	125*	152	164*	180*	192
24	2	32	111	113	182	2*	30*	69	71	79*	81	109*	111*	150*	180*
25	2	8	10	129	163	2*	6*	8*	34*	119*	121	127	153	155*	161*

Stations used :
0 2 4 6 8 10 12 14 16 32 45 64 84 98 100 102 109 110 111 112 113 128 129 140 147 148 163 168 172 173 182 189 190 195 196

Sequences for the 3km minimum redundancy array which have twice and four times the basic increment, that is, 30.612m and 61.224m respectively, are listed below. The double-increment sequence fully fills the 0-3km range (98 baselines in all) in 13 days and the quadruple-increment sequence fills all but one baseline in 8 days. These sequences have not been optimized for uniformity after 4-day intervals or for minimum antenna travel.

Day	Antenna Locations	Baselines									
1	2 98 110 190 196	6	12	80	86	92	96	98	108	188	194
2	6 64 112 182 190	8	48	58	70	78	106	118	126	176	184
3	10 140 172 182 196	10	14	24	32	42	56	130	162	172	186
4	8 128 168 172 190	4	18	22	40	44	62	120	160	164	182
5	0 112 128 148 196	16	20	36	48*	68	84	112	128	148	196
6	0 2 102 140 168	2	28	38	66	100	102	138	140	166	168
7	2 32 84 148 182	30	34	52	64	82	98*	116	146	150	180
8	4 16 98 148 172	12*	24*	50	74	82*	94	132	144	156	168*
9	6 14 102 128 148	8*	20*	26	46	88	96*	114	122	134	142
10	4 10 64 140 168	6*	28*	54	60	76	104	130*	136	158	164*
11	0 12 110 182 190	8*	12*	72	80*	98*	110	170	178	182*	190
12	14 16 100 168 190	2*	22*	68*	84*	86*	90	152	154	174	176*
13	4 16 100 128 196	12*	28*	68*	84*	96*	96*	112*	124	180*	192

Stations used :
0 2 4 6 8 10 12 14 16 32 64 84 98 100 102 110 112 128 140 148
168 172 182 190 196

Day	Antenna Locations	Baselines									
1	0 4 12 100 172	4	8	12	72	88	96	100	160	168	172
2	8 32 112 148 196	24	36	48	80	84	104	116	140	164	188
3	8 64 128 140 172	12*	32	44	56	64	76	108	120	132	164*
4	12 100 140 148 168	8*	20	28	40	48*	68	88*	128	136	156
5	8 100 112 128 172	12*	16	28*	44*	60	72*	92	104*	120*	164*
6	12 16 64 84 196	4*	20*	48*	52	68*	72*	112	132*	180	184
7	12 16 140 168 172	4*	4*	28*	32*	124	128*	152	156*	156*	160*
8	0 4 8 148 196	4*	4*	8*	48*	140*	144	148	188*	192	196

Stations used :
0 4 8 12 16 32 64 84 100 112 128 140 148 168 172 196

A.3 The 6km minimum redundancy array

Day	Antenna Locations	Baselines														
1	12 84 111 129 140 388	11	18	27	29	45	56	72	99	117	128	248	259	277	304	376
2	6 64 112 128 148 392	16	20	36	48	58	64	84	106	122	142	244	264	280	328	386
3	2 32 111 113 189 392	2	30	76	78	79	81	109	111	157	187	203	279	281	360	390
4	14 45 102 168 196 388	28	31	57	66	88	94	123	151	154	182	192	220	286	343	374
5	12 16 109 172 182 392	4	10	63	73	93	97	156	160	166	170	210	220*	283	376*	380
6	4 45 140 163 195 392	23	32	41	55	95	118	136	150	159	191	197	229	252	347	388
7	10 84 110 129 196 392	19	26	45*	67	74	86	100	112	119	186	196	263	282	308	382
8	64 98 110 163 190 388	12	27*	34	46	53	65	80	92	99*	126	198	225	278	290	324
9	100 113 128 172 182 388	10*	13	15	28*	44	54	59	69	72*	82	206	216	260	275	288
10	8 32 148 173 195 388	22	24	25	47	116	140	141	163	165	187*	193	215	240	356	380*
11	10 16 112 147 189 388	6	35	42	77	96	102	131	137	173	179	199	241	276	372	378
12	0 8 98 147 168 392	8	21	49	70	90	98	139	147	160*	168	224	245	294	384	392

Stations used :
0 2 4 6 8 10 12 14 16 32 45 64 84 98 100 102 109 110 111 112
113 128 129 140 147 148 163 168 172 173 182 189 190 195 196 388 392

A.4 The 3km redundant array

Two different sequences for the 3km redundant array are given. The first has mainly long redundant spacings and is the one illustrated in Figure 3.9. The second has mainly short redundant spacings.

Day	Antenna Locations					Baselines									
1	4	100	148	172	196	24	24*	48	48*	72	96	96*	144	168	192
2	0	84	140	168	196	28	28*	56	56*	84	84*	112	140	168*	196
3	147	168	182	189	196	7	7*	14	14*	21	21*	28*	35	42	49
4	0	4	14	189	196	4	7*	10	14*	175	182	185	189	192*	196*
5	0	6	10	172	196	4*	6	10*	24*	162	166	172	186	190	196*
6	0	16	100	147	196	16	47	49*	84*	96*	100	131	147	180	196*
7	0	8	113	148	196	8	35*	48*	83	105	113	140*	148	188	196*
8	0	2	12	172	190	2	10*	12	18	160	170	172*	178	188*	190*
9	0	2	102	109	196	2*	7*	87	94	100*	102	107	109	194	196*
10	0	14	32	168	190	14*	18*	22	32	136	154	158	168*	176	190*
11	0	12	32	128	196	12*	20	32*	68	96*	116	128	164	184	196*
12	0	16	64	163	190	16*	27	48*	64	99	126	147*	163	174	190*
13	0	45	64	173	196	19	23	45	64*	109*	128*	132	151	173	196*
14	0	45	98	140	190	42*	45*	50	53	92	95	98	140*	145	190*
15	0	110	129	163	196	19*	33	34	53*	67	86	110	129	163*	196*
16	0	84	110	173	190	17	26	63	80	84*	89	106	110*	173*	190*
17	0	100	111	190	195	5	11	79	84*	90	95*	100*	111	190*	195

Stations used :
0 2 4 6 8 10 12 14 16 32 45 64 84 98 100 102 109 110 111 113
128 129 140 147 148 163 168 172 173 182 189 190 195 196

Day	Antenna Locations					Baselines									
1	4	100	148	172	196	24	24*	48	48*	72	96	96*	144	168	192
2	0	84	140	168	196	28	28*	56	56*	84	84*	112	140	168*	196
3	147	168	182	189	196	7	7*	14	14*	21	21*	28*	35	42	49
4	0	14	84	12	110	2	12	14*	26	70	72*	84*	96*	98	110
5	0	2	12	16	64	2*	4	10	12*	14*	16	48*	52	62	64
6	0	2	6	32	100	2*	4*	6	26*	30	32	68	94	98*	100
7	0	2	8	84	182	2*	6*	8	76	82	84*	98*	174	180	182
8	0	2	102	109	45	2*	7*	43	45	57	64*	100*	102	107	109
9	0	2	110	168	147	2*	21*	37	58	108	110*	145	147	166	168*
10	0	2	111	140	128	2*	12*	17	29	109*	111	126	128	138	140*
11	0	2	113	129	148	2*	16*	19	35*	111*	113	127	129	146	148
12	0	2	196	172	190	2*	6*	18	24*	170	172	188	190	194	196*
13	0	4	45	84	128	4*	39	41	44	45*	80	83	84*	124	128*
14	0	4	64	110	173	4*	46	60	63	64*	106	109*	110*	169	173
15	0	2	173	163	195	2*	10*	22	32*	161	163	171	173*	193	195
16	0	4	109	129	140	4*	11	20	31	105	109*	125	129*	136	140*

Stations used :
0 2 4 6 8 12 14 16 32 45 64 84 100 102 109 110 111 113 128 129
140 147 148 163 168 172 173 182 189 190 195 196

A.5 The 6km redundant array

Day	Antenna Locations						Baselines														
1	4	100	148	172	196	388	24	24*	48	48*	72	96	96*	144	168	192	192*	216	240	288	384
2	0	84	140	168	196	392	28	28*	56	56*	84	84*	112	140	168*	196	196*	224	252	308	392
3	147	168	182	189	196	388	7	7*	14	14*	21	21*	28*	35	42	49	192*	199	206	220	241
4	10	45	112	168	189	392	21*	35*	56*	67	77	102	123	144*	158	179	203	224*	280	347	382
5	32	84	148	172	189	392	17	24*	41	52	64	88	105	116	140*	157	203*	220*	244	308*	360
6	0	14	98	110	189	392	12	14*	79	84*	91	96*	98	110	175	189	203*	282	294	378	392*
7	8	16	64	147	189	392	8	42*	48*	56*	83	125	131	139	173	181	203*	245	328	376	384*
8	2	6	16	32	111	392	4	10	14*	16	26	30	79*	95	105*	109	281	360*	376*	386	390
9	6	12	98	128	168	392	6	30*	40	70	86	92	116*	122	156	162	224*	264	294*	380	386*
10	4	10	128	163	173	392	6*	10*	35*	45	118	124	153	159	163	169	219	229	264*	382*	388
11	8	128	172	182	195	392	10*	13	23	44	54	67*	120	164	174	187	197	210	220*	264*	384*
12	2	102	113	128	190	392	11	15	26*	62	77*	88*	100	111	126	188	202	264*	279	290	390*
13	12	102	109	111	189	392	2	7*	9	78	80	87	90	97	99	177	203*	281*	283	290*	380*
14	8	100	129	168	173	392	5	29	39	44*	68	73	92*	121	160	165	219*	224*	263	292	384*

Stations used :
0 2 4 6 8 10 12 14 16 32 45 64 84 98 100 102 109 110 111 112
113 128 129 140 147 148 163 168 172 173 182 189 190 195 196 388 392